https://doi.org/10.5194/egusphere-2026-6138
Preprint. Discussion started: 2 November 2026
© Author(s) 2026. CC BY 4.0 License.

Plant nitrogen acquisition strategies impact ecosystem carbon storage under future climate

Gabriela Sophia[1,2,4], Sönke Zaehle[1,3], Benjamin D. Stocker[4,5], Silvia Caldararu[6]

[1] Max Planck Institute for Biogeochemistry, Jena, Germany; [2] International Max Planck Research School on Global Biogeochemical Cycles, Jena, Germany; [3] Friedrich Schiller Universität Jena, Jena, Germany; [4] Geographisches Institut, Universität Bern, Bern, Switzerland; [5] Oeschger Center, Universität Bern, Bern, Switzerland; [6] Discipline of Botany, School of Natural Sciences, Trinity College Dublin, Dublin, Ireland. Correspondence: Gabriela Sophia (gsophia@bgc-jena.mpg.de)

Abstract

Plant nitrogen (N) use strategies affect ecosystem nutrient cycles and limitation and thereby the response of ecosystems to global change. However, their influence on future projections of nutrient limitation and land carbon (C) sink remains unclear. Here, we used a nitrogen-enabled biosphere model (QUINCY) to evaluate the competitiveness of acquisitive (high uptake, low resorption) and conservative (low uptake, high resorption) N-use strategies within plant functional types (PFTs) and climate zones under a scenario of future climate change (SSP3-7.0). We assessed competitive advantage via net primary productivity (NPP) and implications for C storage and N cycling through total ecosystem C and the ecosystem N uptake/loss ratio. Our results suggest that a broad-leaved deciduous (BDS) conservative strategy has a stronger competitive advantage compared to needle-leaved evergreens (NE) conservative, as shown by the largest relative gains in NPP (+48%) and Ecosystem C (+22%) together with smaller increases in N losses (-7.6%). This overall response varies across climate zones reflecting the latitudinal gradient in nutrient limitation. In the tropics, where N is generally not a limiting nutrient, acquisitive and conservative N-use respond similarly. In contrast, temperate and boreal regions sustain a clear advantage for conservative strategies, with higher gains in NPP (+24.8% vs. +18.7% in temperate BDS; +18.8% vs. +17.7% in temperate NE; +41.3% vs. +30.5% in boreal BDS; +56.7% vs. +46.5% in boreal NE), and consistent patterns for C storage. Together, the findings underscore that the functional N-use

https://doi.org/10.5194/egusphere-2026-6138
Preprint. Discussion started: 2 November 2026
© Author(s) 2026. CC BY 4.0 License.

strategy diversity within PFTs may influence future C and N projections, and represents a conceptual step toward improving model realism.

Keywords: Nitrogen-use strategies; Functional diversity; Nitrogen cycling; Carbon cycling; Terrestrial biosphere modeling; Rising CO_2; Nitrogen deposition; ISIMIP projection; Global climate change.

1. Introduction

Terrestrial ecosystems play a critical role in regulating the Earth's climate, currently absorbing nearly 30% of anthropogenic CO_2 emissions each year (Friedlingstein et al., 2024). This carbon (C) sink is tightly coupled with the nitrogen (N) cycle, since N is essential for enzyme formation, supports key metabolic functions such as photosynthesis and cell formation, and is therefore required for biomass production (Chapin 1980; Luo et al., 2004; Zaehle et al., 2010; Wieder et al., 2015b; Caldararu et al., 2021). Strategies by which plants acquire and utilize N not only influence their productivity but also shape broader ecosystem-level processes, such as C sequestration, nutrient cycling, and feedbacks to atmospheric CO_2 and climate (Zaehle et al., 2010; Cambron et al., 2025). As global change accelerates via elevated CO_2, rising temperatures, and shifting patterns of N deposition, it becomes important to understand how N-use plant strategies mediate ecosystem responses toward the end of the 21st century. We define N-use strategies as the combination of external N acquisition (e.g. root uptake and associated pathways) and internal N recycling processes that plants use to meet internal N demand in variable soil conditions, each carrying different energetic and C costs (Shi et al., 2016). However, while models represent major C-N processes, they generally do not distinguish differences in these strategies within or across Plant Functional Types (PFTs), likely underestimating how plants meet internal demand and, ultimately, the land C sink (Cambron et al., 2025). Therefore, its role in influencing future projections of nutrient limitation is yet unclear (Wieder et al., 2015; Zaehle et al., 2015; Stocker et al., 2024).

Most global land surface models use simplified vegetation representations, typically grouping species into PFTs based on broad traits such as leaf habit, type and biome (Fisher and Koven, 2020). This captures major differences across vegetation types (Pretince et al., 2007), but it often masks important within-PFT functional diversity, particularly in how plants acquire

https://doi.org/10.5194/egusphere-2026-6138
Preprint. Discussion started: 2 November 2026
© Author(s) 2026. CC BY 4.0 License.

and use nutrients (Verheijen et al., 2013; Pavlick et al., 2013). In reality, species within the same PFT can vary substantially in their N-use strategies, ranging from conservative that prioritizes internal N recycling over external uptake and investments into root acquisition, to acquisitive strategies that rely more on rapid external uptake with higher root allocation and low internal recycling (Phillips, Brzostek, and Midgley, 2013; Sophia et al., 2024). Acquisitive vs. conservative N-use therefore cannot be simulated simply by differences in e.g. evergreen vs. deciduous fixed PFT.

Resorption is shaped by both leaf traits and environment conditions: species with higher SLA (specific leaf area) and greater investment in metabolic N, such as deciduous plants, generally resorb more efficiently than evergreens, whose thicker leaves contain more structural, non-mobilizable N (Onoda et al., 2017; Sophia et al., 2024). But this potential maximum metabolic-N resorption is down-regulated in response to climate and soils, generally decreasing from arctic to warm-wet tropical regions, where faster nutrient cycling and lower costs of external uptake make N uptake more advantageous (Deng et al., 2018; Estiarte et al., 2023; Sophia et al., 2024). While deciduous species are often considered as more physiologically acquisitive, and evergreens as more conservative based on the global Leaf Economics Spectrum (LES; Wright et al., 2004), both PFTs can adopt either the described acquisitive or conservative N-use, depending on environmental context and nutrient availability.

Under future climate scenarios, these N-use strategies may respond differently. Rising CO_2 may intensify N limitation (Walker et al., 2021), potentially favoring conservative N-use that rely on high internal resorption to sustain net primary productivity (NPP) under progressive increase of N demand (Wieder et al., 2015; Sophia et al., 2026). Conversely, warming stimulates microbial decomposition and mineralization of organic matter, leading to short-term pulses of N (Melillo et al., 2011). These transient increases, on top of rising CO_2 and shifts in N deposition, may favor acquisitive N-use that can maximize uptake capacity and quickly take advantage of this newly accessible N to convert into higher photosynthesis and NPP (Finzi et al., 2007; Norby and Zak, 2011). It is then expected that either acquisitive or conservative N-use ultimately shape ecosystem C storage differently, with cascading implications for nutrient cycling. Predicting which strategy will enhance ecosystem function and show stronger competitive advantage under future conditions is therefore essential for improving realism in model predictions and deepening our insight into ecosystem resilience under global change.

https://doi.org/10.5194/egusphere-2026-6138
Preprint. Discussion started: 2 November 2026
© Author(s) 2026. CC BY 4.0 License.

In this study, we address this gap by explicitly incorporating two distinct N-use strategies - conservative (high resorption, low uptake) and acquisitive (low resorption, high uptake) - within PFTs using the QUINCY terrestrial biosphere model (QUantifying Interactions between terrestrial Nutrient CYcles and the climate system, Thum et al., 2019). We assess the impact of these strategies on future productivity and ecosystem C storage under the changing climate. First, we apply co-located simulations at selected sites where two PFTs (needle-leaved evergreen and broad-leaved deciduous) can coexist, and isolate the effect of N-use strategy within each PFT under identical climate trajectories. We then extend the analysis to a representative set of globally distributed sites across all climate zones, allowing us to quantify the large-scale implications of different N-use strategies. Finally, we include two factorial simulations with fixed CO_2 and N deposition, to disentangle the influence of these drivers on plant strategy outcomes. Our main questions are: **(i)** Which N-use strategy is likely to gain a competitive advantage at the end of the 21st century, and what are the implications for the C and N ecosystem cycling? **(ii)** Are there regional exceptions to the strategy performance on a global-scale, and what is the global picture of C storage? **(iii)** how do rising CO_2 and N deposition drivers modulate the N-use strategies outcomes? For the first question, we measure competitiveness by assessing NPP, while for the implications for C storage, we consider total ecosystem C (with results for vegetation and soil C separately reported in the SI), and evaluate implications for N cycling via the ecosystem uptake loss metric - ratio of plant N uptake to sum of leaching and fluxes of gas loss, in which an increase in this ratio means a more closed N cycle and increasing ecosystem N limitation. For the second question, we scale the analysis across tropical, temperate, and boreal zones, assessing how climate gradients modulate strategy effects on NPP and C storage. Finally, for the third question, we look at the discussed global picture of C storage to disentangle the contributions of different atmospheric drivers.

2. Methods

2.1 QUINCY model description

We briefly describe below the relevant model configuration for representing different N-use strategies. More details can be found in Thum et al., (2019). We ran the model with dynamic allocation, dynamic stoichiometry (Thum et al., 2019), and dynamic resorption (Sophia et al., 2026). These settings allow plants to adjust their biomass partitioning and nutrient ratios in

https://doi.org/10.5194/egusphere-2026-6138
Preprint. Discussion started: 2 November 2026
© Author(s) 2026. CC BY 4.0 License.

response to environmental conditions. QUINCY has 8 PFTs, distinguished by differences in phenology, leaf form, growth strategy, and photosynthetic pathway. In this study, we focused on the woody PFTs broad-leaved summergreen deciduous trees (BDS), moist broad-leaved evergreen trees (BEM), and needle-leaved evergreen trees (NE). These PFTs are more representative of tropical, temperate and boreal forests, and the choice largely aligns with the implemented and tested dynamic nutrient resorption scheme in QUINCY (Sophia et al., 2026).

Dynamic stoichiometry: The leaf N concentration is adjusted according to the relative availability C and N needed for growth, in line with the stoichiometric requirements. This is represented by an empirical representation based on Zaehle and Friend (2010). If plants lack sufficient nutrients relative to the current C:N ratio, the leaf N concentration decreases. Conversely, when N are sufficient, the leaf N concentration increases. Equations can be found in Thum et al., 2019.

Dynamic allocation: Allocation of leaves vs. roots is allowed to vary and responds to growth N demand relative to available N, as well as to water limitation. When N demand exceeds supply, the model increases root allocation to enhance uptake at the expense of leaf and stem growth. Also, under water stress, more biomass is directed to roots to increase water acquisition. Conversely, when these resources are sufficient, allocation shifts toward leaves to support C assimilation and growth. Equations can be found in Thum et al., 2019.

Dynamic N resorption: The dynamic N resorption accounts for both structural and environmental constraints in the maximum resorption capacity (equations can be found in Sophia et al., 2026). The structural limitation reflects the partitioning of leaf N into metabolic and structural fractions, with only the metabolic component considered mobilisable at senescence. This sets an upper bound on resorption that co-varies with leaf construction costs and captures structural differences between PFTs. Accordingly, the expected order across PFTs is: higher resorption in BDS > BEM > NE. This structural maximum is further downregulated by environmental limitation, where the modelled leaf C:N ratio is used as an emergent proxy for N status. Higher leaf C:N indicates stronger N limitation and increases resorption, while sensitivity is reduced under extreme C:N conditions. Together, these constraints allow

https://doi.org/10.5194/egusphere-2026-6138
Preprint. Discussion started: 2 November 2026
© Author(s) 2026. CC BY 4.0 License.

QUINCY to represent both the structural differences in resorption among PFTs and their indirect response to variable N status.

N uptake: In QUINCY, plant N uptake (U_N) from the soil is calculated as a function of fine root biomass, inorganic N availability, and plant nutrient demand, following an extended Michaelis-Menten formulation (more details in Thum et al., 2019). The potential uptake rate of inorganic N (in which N = ammonium [NH_4^+] + nitrate [NO_3^-]) is given by:

$$U_N = v_{max,N}(T_{soil,}\psi) \times N \times (K_{m1,N}(T_{soil,}\Theta) + \frac{1}{K_{m2,N}(T_{soil,}\Theta)+N}) \times f^N_{demand} \times C_{fine-root} \quad \text{(Eq.1)}$$

where $v_{max,N}$ is the PFT-specific maximum uptake rate per unit root biomass, adjusted to soil temperature (T_{soil}) and water potential; $C_{fine-root}$ is the fine root biomass (mol C m^{-3}); K_m parameters represent the nutrient sensitivities of the low and high affinity transporters, adjusted to soil moisture. The factor f^N_{demand} downregulates uptake according to plant internal N demand, based on the ratio of available N to the N required for growth.

2.2 Representation of distinct N-use strategies

We modified the maximum rate of plant mineral N uptake (v_{max}) to represent contrasting plant N-use strategy. This parameter regulates how much N plants can acquire externally, and reflects their reliance on soil N *versus* internal recycling. Changes in v_{max} indirectly alter leaf C:N ratios, which in turn adjust resorption as an emergent response considering the dynamic resorption scheme (Sophia et al., 2026). For example, in our setup, lowering v_{max} reduces soil N uptake, which increases N limitation. This leads to higher leaf C:N ratios, and under the dynamic resorption scheme, higher leaf C:N in turn increases N resorption (see in 3.1 Nitrogen uptake and resorption trends). We defined two strategies by modifying the default model value (0.42 molN m^{-2} day^{-1}) in ±20% equal among PFTs:

https://doi.org/10.5194/egusphere-2026-6138
Preprint. Discussion started: 2 November 2026
© Author(s) 2026. CC BY 4.0 License.

Acquisitive strategy: v_{max} = 0.50 molN m^{-2} day^{-1}. Characterized by high soil N uptake and an emerging behaviour of low N resorption. Represents plants that rely more on external N acquisition to support faster growth and productivity, even under elevated N loss.

Conservative strategy: v_{max} = 0.33 molN m^{-2} day^{-1}. Characterized by low soil N uptake and high N resorption. Reflects species that prioritize internal recycling, favoring efficient internal N use over soil N.

Although v_{max} and resorption are rarely measured together, there is evidence for a trade-off between external N and internal conservation (Deng et al., 2018). This parameter adjustment therefore offers a simple entry point to investigate how differences in N acquisition influence plant productivity, C storage, and ecosystem N cycling under current and future climate conditions. Sensitivity analysis for the parameter adjustment is described in Appendix A1.

2.3 Model setup

We organized our simulations into three main experiments to assess how different N-use strategies interact with plant functional type and climate conditions (Table 1):

(a) Comparative study of N-use strategies under shared climate conditions

Each site is assigned a single predefined PFT according to its dominant vegetation characteristics (Caldararu et al., 2022). In order to understand which of the N-use strategies has an advantage in a future climate, we selected a subset of the global sites where both BDS and NE PFTs can coexist under similar climatic conditions. These sites were used to isolate the effects of PFT identity and N strategy by running each site with both strategies for each PFT. This setup results in four model variants per site (BDS-acquisitive, BDS-conservative, NE-acquisitive, NE-conservative). Site selection criteria were based on overlapping reasonable geographic and climate ranges for both PFTs, found in Appendix A2 (Figs. A3 and A4).

(b) Global study of N-use strategies

In the global experiment, we simulated all sites using their original PFT definitions (Caldararu et al., 2022) including BEM, and ran each site twice - under the acquisitive and conservative

https://doi.org/10.5194/egusphere-2026-6138
Preprint. Discussion started: 2 November 2026
© Author(s) 2026. CC BY 4.0 License.

strategy. This experiment captures large-scale patterns in C storage, productivity, and N cycling that emerge from varying N-use strategies across different climate zones.

(c) Atmospheric driver sensitivity

To isolate the effects of atmospheric drivers on ecosystem processes under differing plant N-use strategies, we ran an additional set of simulations with fixed atmospheric CO_2 and N deposition, both separated but held constant at pre-industrial levels (set to 1850 values) for the entire simulation period (until 2100). This factorial analysis allows us to determine the extent to which rising CO_2 and N deposition influence C and N dynamics under each plant strategy. Temperature and precipitation follow transient pathways in these simulations.

Table 1. Characterization of each experiment conducted in this study.

Experiment	CO_2 fertilization	N deposition	Climate forcing	Site/PFT	N-use strategy	Further features
Comparative N-use strategies	SSP3-7.0	SSP3-7.0	UKESM	BDS and NE co-existing in the same site	Acquisitive Conservative	Each site run with both PFTs and both N-use strategies
Global N-use strategies	SSP3-7.0	SSP3-7.0	UKESM	BDS, BEM and NE original to site	Acquisitive Conservative	One PFT per site based on observed vegetation; all sites simulated globally
Atm driver sensitivity	SSP3-7.0	Fixed (1850)	UKESM	BDS, BEM and NE original to site	Acquisitive Conservative	Used to isolate effect of increasing N deposition
Atm driver sensitivity	Fixed (1850)	SSP3-7.0	UKESM	BDS, BEM and NE original to site	Acquisitive Conservative	Used to isolate effect of CO_2 fertilization
Climate forcing sensitivity	SSP3-7.0	SSP3-7.0	MPI	BDS, BEM and NE original to site	Acquisitive Conservative	Parallel simulations to test model response to different GCM forcing

2.4 Model setup and climate forcing data

We applied the model to 30 grid cells in the comparative study (Fig. A3) and to 124 globally distributed grid cells (Fig. A2), covering a representative distribution of PFTs and climate zones. The daily meteorological forcing for both experiments - disaggregated to half-hourly values using a weather generator (Thum et al, 2019) - was derived from bias-adjusted (Lange, 2019a; Cucchi et al., 2020) outputs of the UKESM1-0-LL global climate model (Sellar et al., 2019), using the SSP3-7.0 emissions scenario - a medium-high reference pathway

https://doi.org/10.5194/egusphere-2026-6138
Preprint. Discussion started: 2 November 2026
© Author(s) 2026. CC BY 4.0 License.

(Meinshausen et al., 2020) (Fig. 1). The dataset spans 1850 to 2100 and includes historical climate (1850-2014) followed by future projections (2015-2100). Climate variables include air temperature, precipitation, solar radiation, relative humidity, wind speed, and surface pressure. Atmospheric CO_2 concentrations follow the historical record until 2014, then track SSP3-7.0 projections. Nitrogen deposition inputs are consistent with the ISIMIP3b scenario, increasing throughout the 20th century before stabilizing under SSP3-7.0 assumptions.

To test the sensitivity of the outcomes to climate forcing, we conducted a parallel set of simulations using climate forcing from the SSP3-7.0 scenario simulation of the MPI-ESM1-2-LR global climate model (Wieners et al., 2019), also bias-corrected using the ISIMIP3b protocol. This comparison allows us to perform a climate sensitivity different to UKESM1-0-LL and assess how model responses vary under different climate trajectories, found in Appendix C.

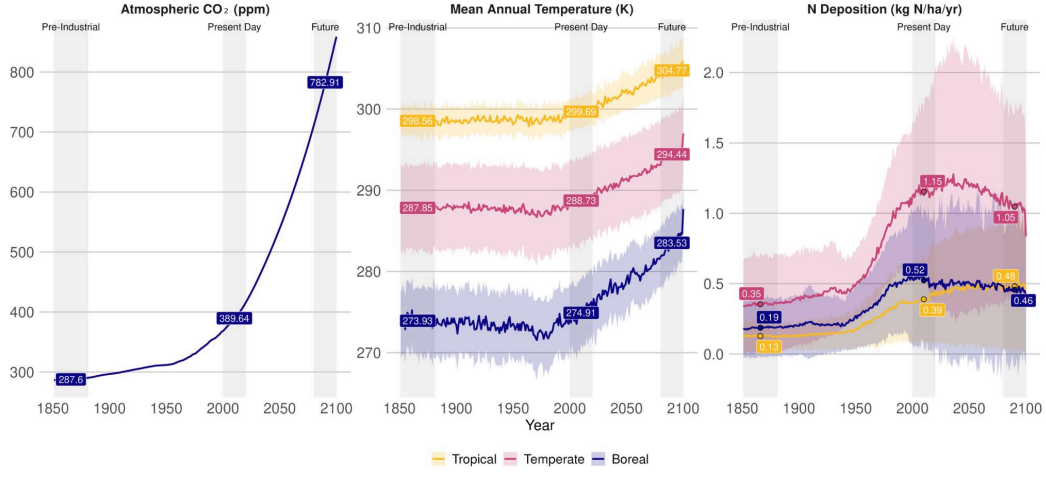


Figure 1: Climate trajectory of atmospheric CO_2 (ppm), Mean Annual Temperature (MAT) and N Deposition (kgN ha/yr) separated in Tropical, Temperate and Boreal climate zones by Köppen climate classification, for the global simulations (124 sites). Pre-industrial (1850-1880), present-day (2000-2020), and future (2080-2100).

2.5 Data analysis

We grouped the temporal trend into Pre-industrial (1851-1881), Present-day (2000-2020), and Future (2080-2100) periods. For each period, we averaged the values over all years. We calculated percentage normalized differences between the Future and Present-day for each model run to assess relative changes in C and N variables, and propagated the standard

https://doi.org/10.5194/egusphere-2026-6138
Preprint. Discussion started: 2 November 2026
© Author(s) 2026. CC BY 4.0 License.

deviation to account for uncertainty. We extracted the present-day Köppen climate classification using the {Kgc} R package (Bryant et al., 2017) for each latitude and longitude. To quantify the contribution of CO_2, N deposition, and the remaining climatic factors in total ecosystem C (ΔEcoC), we compared the change between the future and present day for each N-use strategy runs across three setups: the default simulation with all drivers running dynamically, CO_2-fixed and N deposition-fixed. The CO_2 effect was calculated as the difference in ΔEcoC between the default and CO_2-fixed simulations. The N deposition effect was calculated as the difference in ΔEcoC between the default and N deposition-fixed simulations. The remaining change is then attributed to other drivers.

3. Results

3.1 Nitrogen uptake and resorption trends

The implemented parameter adjustment successfully reproduces the contrast between acquisitive and conservative N-use strategies. Figure 2 shows the temporal trends under SSP3-7.0 scenario in N uptake and leaf N resorption fraction across three time periods (pre-industrial, present day, and future), separated by PFTs and N-use strategies, for the comparative experiment. As expected from the formulation of dynamic nutrient resorption, broad-leaved deciduous (BDS) generally shows higher resorption than needle-leaved evergreen (NE), and acquisitive strategies exhibit higher N uptake and lower resorption compared to conservative strategies within both BDS and NE PFTs across all time periods.

Across all groups, N uptake increases over time, while resorption tends to decline. For BDS acquisitive, N uptake rises from 7.44 ± 0.47 $gN/m^2/yr$ (mean ± SD) in the present day (2000-2020) to 10.31 ± 0.74 in the future (2080-2100), while resorption declines from 0.68 (unitless) ± 0.01 to 0.64 ± 0.02. BDS conservative shows an increase in uptake from 6.13 ± 0.35 $gN/m^2/yr$ to 8.9 ± 0.54 and a slight decrease in resorption from 0.72 ± 0.0 to 0.7 ± 0.01. NE acquisitive increases uptake from 7.09 ± 0.33 $gN/m^2/yr$ to 9.16 ± 0.45, with resorption decreasing from 0.46 ± 0.01 to 0.41 ± 0.01. NE conservative follows a similar trend, with uptake increasing from 6.64 ± 0.30 $gN/m^2/yr$ to 8.64 ± 0.45 and resorption decreasing from 0.51 ± 0.01 to 0.45 ± 0.01.

https://doi.org/10.5194/egusphere-2026-6138
Preprint. Discussion started: 2 November 2026
© Author(s) 2026. CC BY 4.0 License.

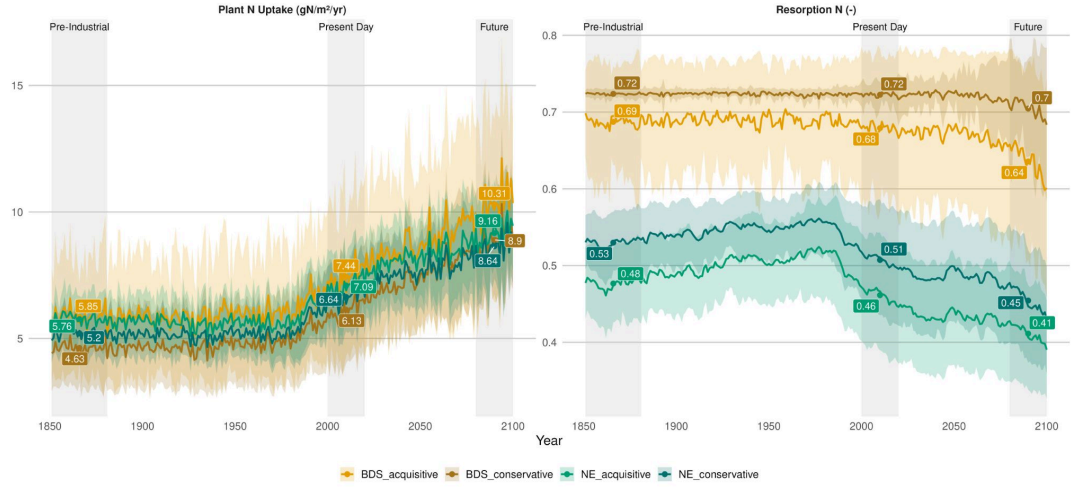


Figure 2: Temporal trends of Plant nitrogen (N) uptake (gN/m^2/yr) and Resorption N (unitless) from 1850 to 2100, based on ISIMIP3b UKESM climate forcing, for the comparative experiment. Different colors show simulations for each plant functional type (broad-leaved deciduous [BDS] and needle-leaved evergreen [NE]) under acquisitive and conservative N-use strategies. The shaded area represents the standard deviation across the 30 sites. Values represent mean annual estimates for each defined period: pre-industrial (1850-1880), present-day (2000-2020), and future (2080-2100).

3.2 Competitive advantage of N-use strategies and its impacts for future C storage and N cycling

To answer the first question on which N use strategy gains most in a future climate, Fig. 3 shows normalized changes (%) from present to future for NPP, total ecosystem C and ecosystem uptake loss (N uptake / Loss) across PFTs and N-use strategies for the comparative experiment. Here, we assess competitive advantage by comparing NPP responses, evaluate the implications for long-term C storage using total ecosystem C, and analyze N cycling efficiency through the ecosystem uptake loss metric. Overall, differences between PFTs are larger than between strategies under the future scenario, with the highest advantage for BDS and conservative strategies based on future mean increases.

The relative gain in net productivity increases across all groups, specially more in BDS strategies, with higher NPP for BDS conservative (48.3% ± 24.8%) and BDS acquisitive (36.7% ± 15.6%), followed by NE conservative (30.1% ± 7.1%) and NE acquisitive (26.9% ± 6.0%). Total ecosystem C also increases across all groups, with BDS conservative showing the

https://doi.org/10.5194/egusphere-2026-6138
Preprint. Discussion started: 2 November 2026
© Author(s) 2026. CC BY 4.0 License.

highest gain (+22.5% ± 9.4%), followed by NE conservative (+18.9% ± 1.9%), BDS acquisitive (+18.6% ± 5.2%) and NE acquisitive (+15.9% ± 1.6%). In contrast, NE acquisitive and NE conservative show the strongest declines in N Uptake/Loss (-48.1% ± 47.3% and -41.9% ± 35.1%, respectively), followed by BDS acquisitive (-23.0% ± 20.1%) and BDS conservative (-4.5% ± 3.9%). Total ecosystem C separated into vegetation and soil C can be found in Fig. B1.

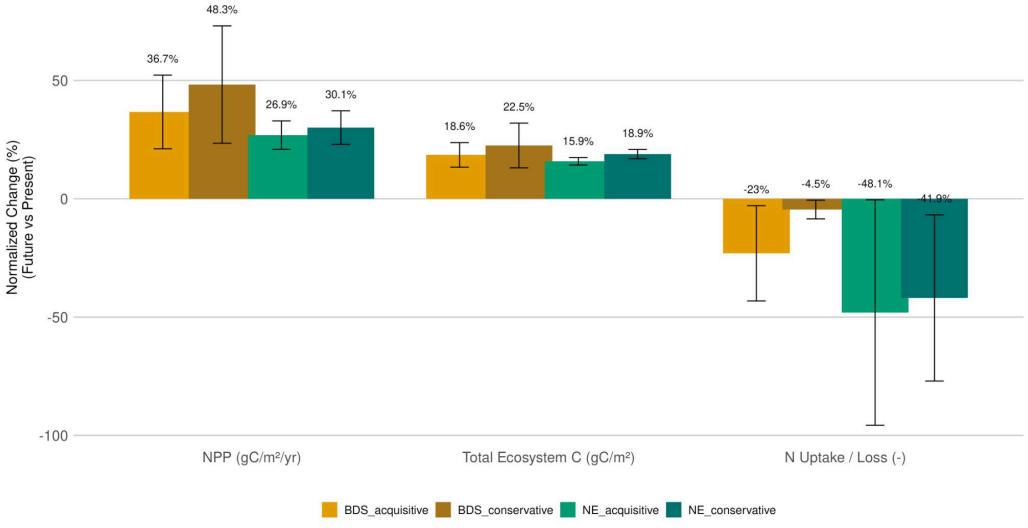


Figure 3: Normalized Change (%) between Future and Present day for Net Primary Productivity (NPP; gN/m^2/yr), total ecosystem carbon (C) (gC/m^2) and N Uptake / Loss (unitless). Bars represent the percent normalized difference and error bars indicate the propagated standard deviation (SE). Different colors show simulations for each plant functional type (broad-leaved deciduous [BDS] and needle-leaved evergreen [NE]) under acquisitive and conservative N-use strategies.

Figure 4 shows the absolute values of NPP, total ecosystem C, and ecosystem uptake loss (N uptake/Loss) through temporal trends under the SSP3-7.0 scenario, across three time periods (pre-industrial, present day, and future), separated by PFTs and N-use strategies for the comparative experiment.

Across all groups, NPP and total ecosystem C increase from present to future, while Ecosystem uptake/Loss declines, indicating more N escaping the system under future conditions. NE shows the highest absolute NPP values in the future, increasing from 714.01 ± 28.04 to 928.8 ± 33.54 gC/m^2/yr for conservative N-use, and from 726.57 ± 27.38 to 922.01 ± 33.15 gC/m^2/yr

https://doi.org/10.5194/egusphere-2026-6138
Preprint. Discussion started: 2 November 2026
© Author(s) 2026. CC BY 4.0 License.

for acquisitive N-use. For BDS, NPP rises from 510.32 ± 31.80 to 697.64 ± 41.22 gC/m^2/yr in acquisitive, and from 427.15 ± 28.0 to 633.32 ± 37.67 gC/m^2/yr in conservative strategies. These increases in net productivity translate into higher total ecosystem C stocks. NE acquisitive increases from 34524.15 ± 330.11 to 40000.27 ± 246.42 gC/m^2, while NE conservative rises from 32795.86 ± 377.79 to 38992.9 ± 312.96 gC/m^2. BDS acquisitive increases from 22118.9 ± 261.82 to 26224.67 ± 319.82 gC/m^2, and BDS conservative from 17123.09 ± 243.03 to 20981.9 ± 349.23 gC/m^2. In contrast, Ecosystem uptake/Loss declines for all groups. BDS acquisitive decreases from 21.63 ± 1.44 to 16.64 ± 1.94, NE acquisitive from 20.76 ± 1.94 to 10.78 ± 1.76, NE conservative from 16.21 ± 1.23 to 9.42 ± 1.37, and BDS conservative from 15.98 ± 0.96 to 15.26 ± 1.62. Total ecosystem C separated into vegetation and soil C can be found in Fig. B2.

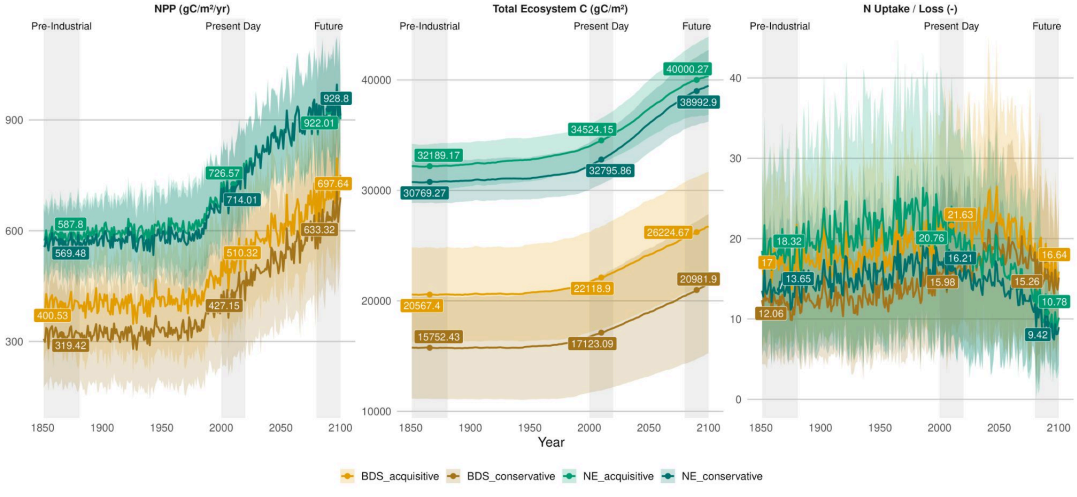


Figure 4: Temporal trends of Net Primary Productivity (NPP; gN/m^2/yr), total ecosystem carbon (C) (gC/m^2) and N Uptake / Loss (unitless), from 1850 to 2100, based on ISIMIP3b UKESM climate forcing, for the comparative experiment. Different colors show simulations for each plant functional type (broad-leaved deciduous [BDS] and needle-leaved evergreen [NE]) under acquisitive and conservative N-use strategies. The shaded area represents the standard deviation across the 30 sites. Values represent mean annual estimates for each defined period: pre-industrial (1850-1880), present-day (2000-2020), and future (2080-2100).

3.3 Global-scale C storage responses to N-use strategies across climate zones

https://doi.org/10.5194/egusphere-2026-6138
Preprint. Discussion started: 2 November 2026
© Author(s) 2026. CC BY 4.0 License.

To answer the second question and test whether N-use strategies perform consistently worldwide or show regional exceptions, we looked at productivity and ecosystem C by PFT across climate zones. This gives the global picture of how strategy differences affect C storage. Figure 5 shows normalized changes (%) from present to future for NPP and total ecosystem C storage across climate zones, PFTs and N-use strategies. NPP hardly changes in the tropics, with both acquisitive and conservative N-use showing slight declines (-0.5 ± 0.2% and -0.2 ± 0.1% in BEM). Conservative strategies consistently outperform acquisitive ones. In temperate regions, NPP in BDS rises by +24.8% ± 7.7% compared to +18.7% ± 5.9% for acquisitive N-use; in BEM, +11.3% ± 3.7% versus +8.4% ± 2.7%; and in NE, +22.7% ± 5.4% versus +21.9% ± 4.9%. The largest gains for conservative appear in boreal regions, where NPP increases by +41.3% ± 13.1% for conservative strategies and +30.5% ± 9.6% for acquisitive ones in BDS. In boreal NE, conservative N-use changes NPP in +56.7% ± 16.1% compared to acquisitive ones +46.5% ± 11.5%. The consequence for total ecosystem C is an increase across all groups, with tropical zones showing the lowest change between N-use strategies (conservative +7.1% ± 2.2 versus acquisitive +6.3% ± 1.9 in BEM). We see the strongest differences between N-use in temperate and boreal regions, particularly in BDS, where conservative strategies show the highest gain (temperate: +21.8% ± 4.6%; boreal: +22.2% for ± 5.7%) compared to acquisitive (+15.7% ± 3%; boreal: +17.5% ± 3.8%). We observe a similar trend in boreal NE, with conservative strategies showing +20.4% ± 4.5% and acquisitive +17.3% ± 2.6%. NE in temperate zones shows smaller changes between N-use strategies (acquisitive: +17.7% ± 4.1%; conservative: +18.8% for ± 4.2%), while BEM shows higher changes for conservative as well (+14.0% ± 5.2%) than acquisitive (+10.8% ± 4%). In these higher-latitude systems, conservative strategies consistently perform better than acquisitive ones for both NPP and total ecosystem C, with little changes in the tropics.

https://doi.org/10.5194/egusphere-2026-6138
Preprint. Discussion started: 2 November 2026
© Author(s) 2026. CC BY 4.0 License.

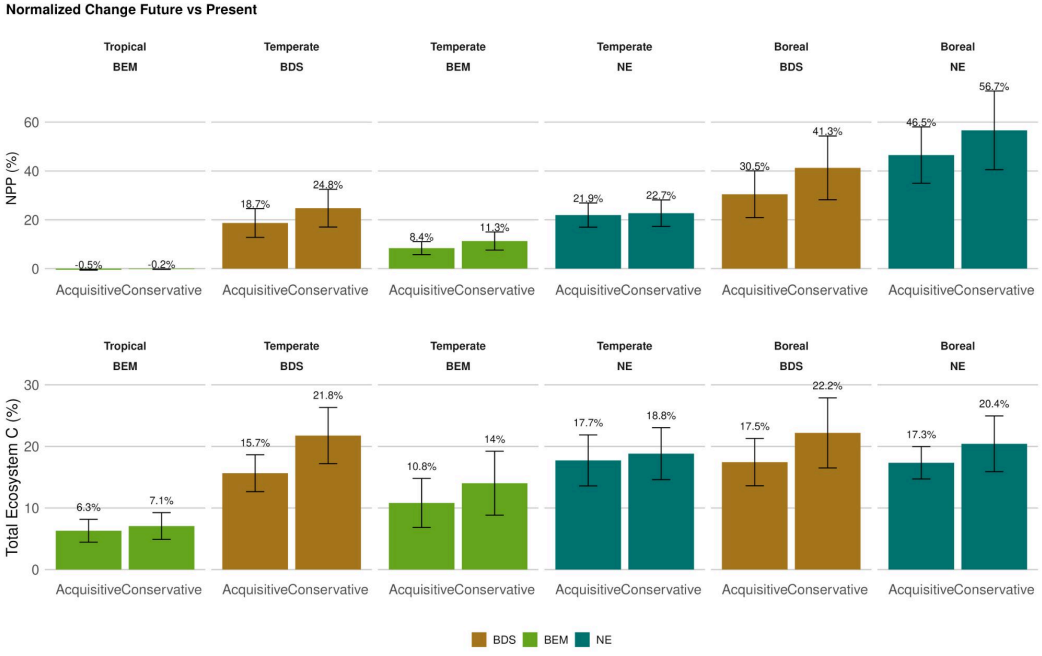


Figure 5: Normalized Change (%) between Future and Present day for NPP (Net Primary Productivity; $gC/m^2/yr$) and total ecosystem carbon (C) (gC/m^2), across climate zones, plant functional types (PFTs) and nitrogen-use strategies (Acquisitive and Conservative). Bars represent the percent normalized difference and error bars indicate the propagated standard deviation (SD). Sites are grouped by Köppen climate classification in Tropical, Temperate, and Boreal zones. Different colors represent each PFT: broad-leaved deciduous (BDS), broad-leaved evergreen (BEM), and needle-leaved evergreen (NE).

Figure 6 shows future total ecosystem C storage across climate zones, N-use strategies, and PFTs for the global experiment. In the tropics, there is minimal difference between strategies: BEM acquisitive stores 27 ± 7 kgC/m², while BEM conservative stores 27 ± 7 kgC/m². In temperate zones, we see a clear difference among PFTs while strategy effects are more pronounced within BDS, where acquisitive store 29 ± 4 kgC/m², compared to 26 ± 4 kgC/m² for conservative. BEM and NE show slight changes between N-use strategies (BEM acquisitive: 33 ± 13 kgC/m², BEM conservative: 32 ± 13 kgC/m²; NE acquisitive: 34 ± 7 kgC/m²; NE conservative: 35 ± 6 kgC/m²). In the boreal zones, both PFT and strategy influence ecosystem C. NE acquisitive shows the highest C storage overall (39 ± 4 kgC/m²), followed by NE conservative (37 ± 6 kgC/m²). For BDS, acquisitive stores 28 ± 4 kgC/m², while conservative

https://doi.org/10.5194/egusphere-2026-6138
Preprint. Discussion started: 2 November 2026
© Author(s) 2026. CC BY 4.0 License.

stores 24 ± 4 kgC/m². Overall, boreal ecosystems consistently store more C than temperate and tropical zones (Fig. B5), but they also hold the largest store in soils (Fig. B6).

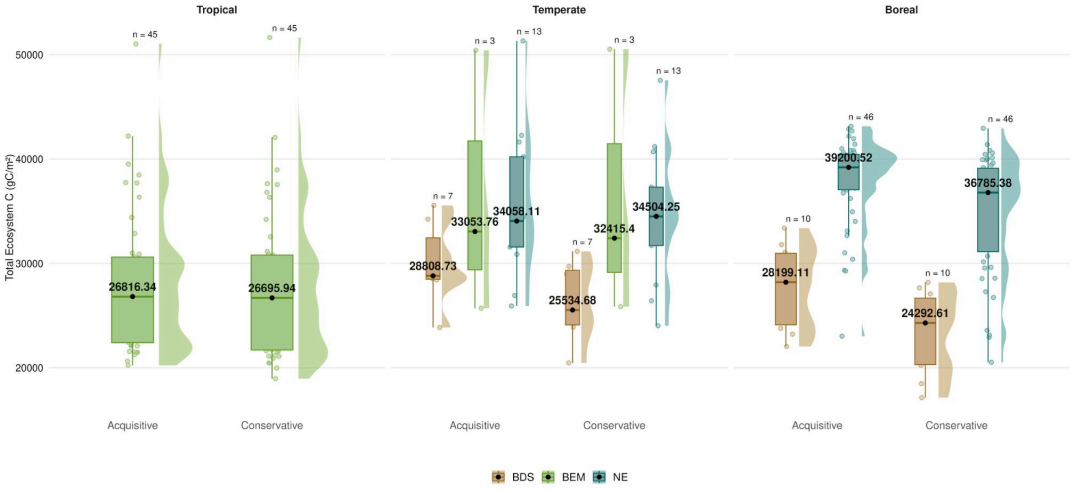
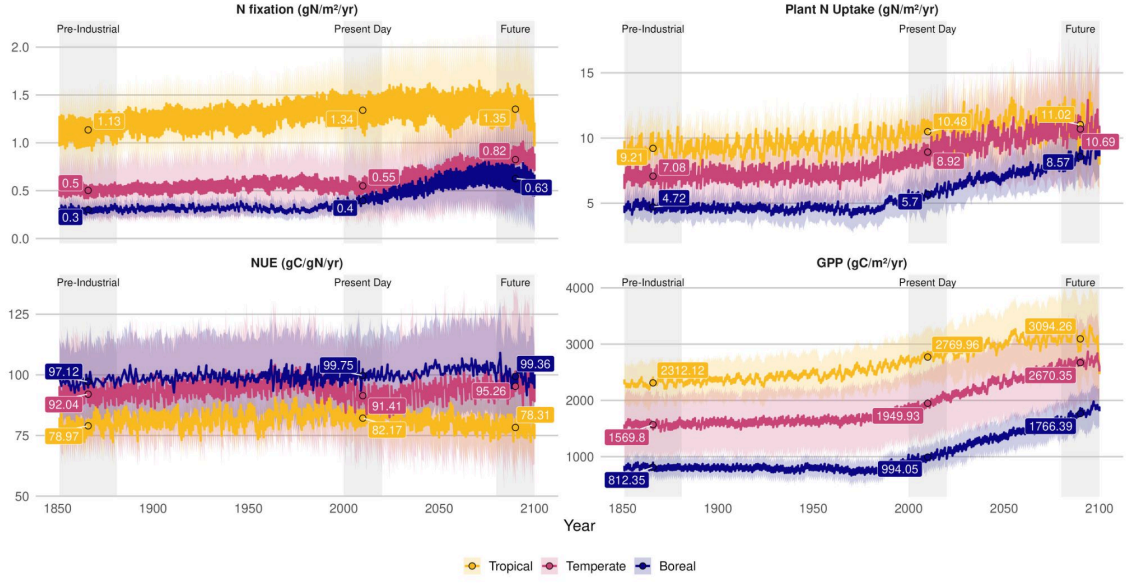


Figure 6: Boxplots show the global distribution of total ecosystem carbon (C) storage (gC/m²) across climate zones and plant functional types (PFTs), for the future period 2080-2100 under two nitrogen-use strategies (acquisitive and conservative). Sites are grouped by Köppen climate classification in Tropical, Temperate, and Boreal zones. Different colors represent each PFT: broad-leaved deciduous (BDS), broad-leaved evergreen (BEM), and needle-leaved evergreen (NE). Boxplots display the median (black dots), interquartile range, and outliers, with side density plots illustrating the overall distribution of values within each group. The number of observations (n) is shown above each box.

To explore how climate zones shape baseline ecosystem functioning under future conditions, independent of N-use strategy differences, Fig. 7 shows the temporal trends in ecosystem variables across tropical, temperate, and boreal regions from 1850 to 2100. We look at biological N fixation, plant N uptake, N-use efficiency production (NUE; ratio of NPP to plant uptake, indicating the biomass production per unit N taken up), and gross primary productivity (GPP). Together, these patterns illustrate how climate-driven differences in N availability and productivity set the context within which N-use strategies operate across regions. Tropical regions show higher rates of biological N fixation, with a marginal increase from 1.34 gN/m2/yr in the present to 1.35 gN/m2/yr by the end of the century. In comparison, temperate regions rise from 0.55 to 0.82 gN/m2/yr, and boreal regions from 0.40 to 0.63 gN/m2/yr. Plant N uptake follows the same pattern, with the tropical zones rising marginally from 10.48 to

https://doi.org/10.5194/egusphere-2026-6138
Preprint. Discussion started: 2 November 2026
© Author(s) 2026. CC BY 4.0 License.

412 11.02 gN/m2/yr, while temperate and boreal increase from 8.92 to 10.69 gN/m2/yr, and 5.70 to
413 8.57 gN/m2/yr from present to future scenario. Considering the higher N availability in the
414 tropics, NUE is consistently lower throughout the years (78.84 gC/gN/yr by the end of the
415 century) compared to 92.98 in temperate and 99.36 in boreal regions. While GPP shows the
416 expected highest values in the tropics across the period, increasing from 2300.47 to 3045.74
417 gC/m2/yr, followed by temperate (1649.23 to 2787.72) and boreal (812.35 to 1766.39) zones.



419 **Figure 7:** Temporal trends of nitrogen (N) fixation (asymbiotic+symbiotic, gN/m^2/yr), Plant N Uptake
420 (gN/m2/yr), NUE (N use efficiency; gC/gN/yr), and (Gross Primary Productivity; gC/m^2/yr) from 1850 to 2100,
421 based on ISIMIP3b UKESM climate forcing. Different colors show different climate zones (Tropical, Temperate,
422 Boreal). Shaded area represents the standard deviation across the 124 global sites. Values represent mean annual
423 estimates for each defined period: pre-industrial (1850-1880), present-day (2000-2020), and future (2080-2100).
424

425 **3.4 Effects of atmospheric drivers on total ecosystem C storage**

426 To address the question on how rising CO_2 and N deposition modulate the outcomes of
427 acquisitive *vs.* conservative N-use strategies, Fig. 8 shows the effects of CO_2 fertilization, N
428 deposition, and other climate drivers (...) on total ecosystem C storage across climate zones and
429 PFTs. Overall, rising CO_2 is the dominant contributor to C gains, with smaller contributions
430 from N deposition and other drivers. In tropical regions, acquisitive and conservative strategies
431 show similar but substantial increases from rising CO_2 (8 kgC/m², respectively), while N

https://doi.org/10.5194/egusphere-2026-6138
Preprint. Discussion started: 2 November 2026
© Author(s) 2026. CC BY 4.0 License.

deposition effects are minimal. Temperate regions show the largest overall C gains, especially in BEM and NE, which increases by 10 kgC/m² and 9 kgC/m² for conservative and acquisitive. For both PFTs, N deposition effects remain small. BDS shows lower gains from rising CO_2 (6 kgC/m² acquisitive; 5 kgC/m² conservative) but a stronger relative contribution from N deposition (1.4 kgC/m² conservative; 0.6 kgC/m² acquisitive). In boreal regions, total C gains are smaller than in temperate zones, but N deposition plays a larger role for BDS. NE acquisitive gains 8 kgC/m² from rising CO_2 with marginal effects from N deposition, while NE conservative gains 7 kgC/m² from rising CO_2 and 0.4 kgC/m² from N deposition. BDS acquisitive gains 5 kgC m^2 from rising CO_2 and 1 kgC/m² from N deposition, while BDS conservative gains 4 kgC/m² from rising CO_2 and 3 kgC/m² from N deposition.

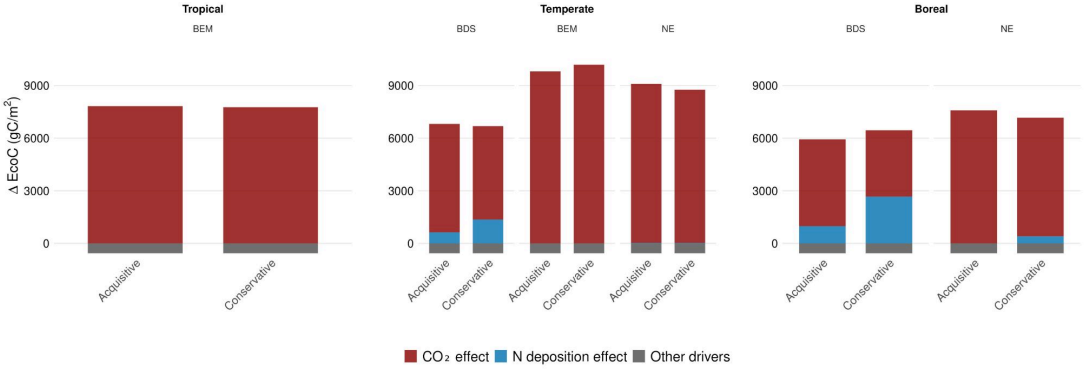


Figure 8: Bars show the change in total ecosystem carbon (ΔEcoC; Future - Present day) separated by N-use strategy and plant functional type (PFT) within each climate zone, using the UKESM climate model. Colors indicate the estimated contribution from each driver: N deposition, CO_2, and other drivers. Driver contributions were calculated by comparing the normal run (all factors varying) with experimental runs where either CO_2 concentration or N deposition was held constant. CO_2 effect = ΔEcoC(normal) - ΔEcoC(CO_2 fixed); N deposition effect = ΔEcoC(normal) - ΔEcoC(N deposition fixed); Other drivers = ΔEcoC(normal) - (CO_2 effect + N deposition effect).

4. Discussion

This study applies a process-based model to evaluate how different N-use strategies shape C storage under the future climate across PFTs and climate zones. By simply adjusting N uptake capacity parameter - that indirectly triggers a response in N resorption, we capture the trade-off between acquisitive and conservative N-use strategies, and how they interact with PFT structural traits. Across all simulations, NPP increases primarily in response to rising CO_2,

https://doi.org/10.5194/egusphere-2026-6138
Preprint. Discussion started: 2 November 2026
© Author(s) 2026. CC BY 4.0 License.

while N losses also increase, leading to a more open N cycle under future conditions. Among BDS, the conservative strategy shows the strongest advantage (in terms of NPP increase) over the acquisitive strategy, with higher C storage and efficient N retention in terms of N uptake/loss ratio. Among other PFTs, the differences are smaller. Conservative N-use with BDS traits allows internal recycling to maintain growth and slow N cycling, while still benefiting from fast soil N releases through higher mineralization. This shift is sustained particularly in non-tropical regions where the whole of N in productivity increases and N-use strategies have a stronger influence. These findings highlight that using only broad PFT categories in land surface models (LSMs) can miss important functional differences within-PFT, as well as the need to include functional trait diversity to better predict the ecosystem responses and terrestrial C sink under climate change.

4.1 N-use strategies and PFT differences

In this study, we tested which N-use strategy is likely to gain a competitive advantage at the end of the 21st century under identical climate trajectories, and what are the implications for the C ecosystem balance and N cycling. Across all simulations, NPP increases towards the future, at the same time, the N uptake/loss ratio declines, indicating an excess of mineral N not assimilated by plants and therefore more prone to gaseous losses and leaching (Fig 4). The key question was therefore whether acquisitive or conservative N-use strategies would be better suited to these future conditions. Our results show a clear distinction between absolute ecosystem performance and relative response to climate change.

The comparative experiment shows that NE acquisitive holds the highest absolute NPP and total ecosystem C storage (Fig. 4), while BDS conservative shows the largest relative gains in NPP and C stocks between present and future climates (Fig. 3). This pattern is reinforced by the global analysis, where BDS conservative achieves the largest percentage increases across climate zones (Fig. 5), while NE acquisitive consistently stores the most C (Fig. 6). This means that acquisitive strategies dominate in terms of absolute productivity and C storage, while conservative strategies respond more strongly relative to the present-day.

Warming and rising CO_2 stimulate microbial activity and N mineralization, increasing soil N availability (Melillo et al., 2011; Sistla et al., 2013). In the model, both stimulate higher soil temperature and consequently microbial activity, with enhanced N mineralization (Figs. B2 and B4), and especially N fixation that adds N to get recycled and mineralized again, accelerating

https://doi.org/10.5194/egusphere-2026-6138
Preprint. Discussion started: 2 November 2026
© Author(s) 2026. CC BY 4.0 License.

N losses (Fig. B4) despite the slight decrease in N deposition in the future (Fig. 1; Zhu et al., 2025). This accumulation of N from deposition and additional N input from faster soil N cycling supports higher GPP and vegetation C storage (Figs. B1 and B2) across all sites.

Acquisitive strategies then benefit from higher plant N uptake capacity, which allows them to quickly use potential short-term soil N releases under warming conditions. When acquisitive N-use is combined with NE structural traits, the result is the highest absolute NPP and ecosystem C storage (Fig. 4). Needle-leaved evergreens are characterized by longer leaf lifespans, high wood investment, low turnover rates, and large structural biomass pools (Reich, 2014), which extend C residence time. This means that NE acquisitive can capitalize on transient N inputs but also retain the C gained for longer periods, resulting in the highest absolute ecosystem and soil C stocks across sites. However, acquisitive strategies also show the strongest declines in the N uptake/loss ratio (Figs. 3 and 4), indicating that faster N cycling and rapid uptake of newly available N is also linked to greater relative increase in N losses under future climate conditions (Fig. B3).

In contrast, conservative strategies show stronger relative competitive advantage (NPP gains) and ecosystem C storage under future climates (Figs. 3 and 5). Although the model does not simulate competition explicitly, e.g. through demographic processes or size-dependent resource acquisition, we use NPP as a measured metric for competitive advantage (Grime, 1998) as it reflects the capacity of each strategy to capture resources and sustain growth under future conditions. Conservative N-use is characterized by high N resorption and more efficient internal recycling (Sophia et al., 2026), which reduces dependence on rapid external N acquisition and allows productivity gains to be sustained despite increasing N losses from the system. In face of that, conservative strategies also show smaller declines in the N uptake/loss ratio (Figs. 3 and 4), indicating tighter N retention under the overall acceleration of N cycling in the model. Therefore, higher resorption appears to buffer part of this effect by slowing the transfer of N through the plant-soil system. As a result, less N is lost from the system relative to plant uptake when compared to acquisitive strategies (Fig. B3). The combination of conservative N-use with BDS traits amplifies this relative advantage. Broad-leaved deciduous have higher tissue turnover and lower baseline biomass than NE (Reich, 2014), which likely allows faster structural and physiological adjustments to climate-driven changes in nutrient cycling - as represented in the model to some extent, and therefore, respond more strongly in relative terms (Figs. 3, 5 and B1).

https://doi.org/10.5194/egusphere-2026-6138
Preprint. Discussion started: 2 November 2026
© Author(s) 2026. CC BY 4.0 License.

Overall, the results suggest that while acquisitive strategies through external uptake maximize absolute productivity and C storage by rapidly exploiting newly available N, conservative strategies through higher resorption show stronger relative competitive advantage because tighter internal recycling and higher N retention sustain productivity and reduce the proportion of N lost from the system.

4.2 Global climate gradients of N-use impacts

The global analysis extends these patterns and highlights how climate zones shape the role of N-use strategies in C storage responses. In general, we simulate a stronger influence of N-use strategy in boreal and temperate regions where N limitation is more pronounced (Figs. 5 and 6), while in the tropics, the lack of difference between strategies likely reflect the high N availability limiting its role in determining C storage.

Boreal zones hold the largest absolute total ecosystem C, particularly in NE acquisitive under future conditions (Fig. 6). This reflects the large soil C pools that dominate boreal systems (Fig. B6), a consequence of slow decomposition rates in cold soils that allow soil organic matter (SOM) to accumulate over centuries (Schmidt et al., 2011; Bradford et al., 2016), which is sustained by long-lived evergreen biomass (Bonan, 2008). While N fixation and uptake are relatively low compared to temperate and tropical regions, boreal systems maintain the highest NUE (Fig. 7), relying more on internal N cycling to meet nutrient demand. Their large absolute C stocks in NE acquisitive in boreal are primarily the result of slow decomposition, high soil C accumulation, and long-lived woody biomass. Under warming, longer growing seasons can stimulate microbial mineralization (Melillo et al., 2011; Sistla et al., 2013), allowing acquisitive strategies to make use of short-term increases in available N, whereas conservative strategies remain in advantage by retaining N under shifts in N cycling, as discussed in the previous section.

Temperate zones store less C than boreal forests but exhibit greater variability among PFTs. These regions have higher annual GPP and N uptake than boreal forests (Fig. 7) due to warmer growing conditions, but these conditions also accelerate SOM decomposition and lead to faster C turnover with lower accumulation of long-lived biomass and soil C (San Román et al., 2024). Within this climate context, structural investment patterns explain some PFT differences: NE shows the highest total ecosystem C (Fig. 5), consistent with its longer tissue residence times and higher structural biomass. BDS and BEM generally show lower C stocks, reflecting faster

https://doi.org/10.5194/egusphere-2026-6138
Preprint. Discussion started: 2 November 2026
© Author(s) 2026. CC BY 4.0 License.

turnover and lower long-term biomass accumulation of broad-leaved plants relative to NE. However, the representation of BEM is based on a limited number of sites, which constrains robust comparison. Relative gains, however, are again greater in BDS conservative (Fig. 5) that can respond rapidly to shifting N availability through faster tissue turnover, combined with high N retention that supports productivity and reduces the proportion of N lost from the system in face of simulated future conditions.

On the other hand, tropical zones show the lowest absolute total ecosystem C (Fig. 6) and minimal differences between strategies or PFTs in relative terms (Fig. 6). These regions sustain the highest GPP, N fixation, and N uptake globally, combined with the lowest NUE (Fig. 7), reflecting consistently high N availability. In addition, the abundance of N-fixing species in the tropics (Fig. 7; Hedin et al., 2009) reduces the reliance on internal N conservation (Cleveland et al., 2013) and may limit the influence of N-use strategy on C storage outcomes. This is in agreement with observations that phosphorus, not N limitation, is prevalent on older soils in warm climates (Walker and Syers, 1976; Vitousek et al., 2010). It is likely that if we were to repeat this model experiment using P-use strategies, we would see similar patterns across a P acquisitive vs conservative spectrum.

Across all climate zones, rising CO_2 is the dominant driver of total ecosystem C gains (Fig. 8), consistent with the widely observed capacity to primarily boost photosynthetic activity (Norby et al., 2005; Ainsworth and Long, 2005). In tropical regions, high N availability from biological N fixation and faster cycling means that N deposition has marginal effects, and therefore both acquisitive and conservative strategies respond similarly to CO_2 fertilization. Toward higher latitudes, the relative contribution of N deposition increases, particularly for BDS conservative in boreal systems, where high NUE means less N inputs can strongly influence productivity. Temperate regions show the largest absolute C gains, especially in high-biomass PFTs such as BEM and NE, while N deposition effects are again pronounced in BDS conservative. These patterns align with the latitudinal gradient in N limitation, as well as with the discussed combination of faster tissue turnover that may allow rapid adjustment to environmental changes while high N retention sustains productivity. This combination makes them more responsive to N deposition in absolute terms, and more competitive where efficient N retention becomes increasingly important to sustain productivity and reduce N losses, particularly in boreal and temperate zones where N retention plays a critical role in the total primary production (Cleveland et al., 2013). The sensitivity experiment with the

https://doi.org/10.5194/egusphere-2026-6138
Preprint. Discussion started: 2 November 2026
© Author(s) 2026. CC BY 4.0 License.

MPI-ESM1-2-LR forcing simulates a lower warming trajectory in the future when compared to UKESM1-0-LL (Fig. C1) and reduces the negative climate effect on C storage (Fig. C2). It also simulates a relatively stronger contribution of N deposition on C storage (Fig. C2), which can be an effect of lower temperatures decreasing mineralization, that lately may increase ecosystem sensitivity to external N inputs. Importantly, despite these expected general differences in climate forcing, the main conclusions regarding the relative performance of N-use strategies should remain robust.

4.3 Plant strategies vs. PFT representations

Our results demonstrate that a parameter adjustment to simulate trait variation within PFTs - here represented by differences in N-use strategies - can significantly alter projections of ecosystem C storage and nutrient cycling under future climate conditions. These differences would be masked if each PFT were represented by the original single average parameterization. It is known that functional diversity plays an important role in shaping ecosystem functioning and how it responds to environmental changes (Díaz and Cabido, 2001; Reich, 2014; Díaz et al., 2016; Cadotte, 2017). Studies show that e.g. rising CO_2 can alter species composition in grasslands (Zelikova et al., 2014) and boreal peatlands (McPartland et al., 2020), with modeling studies also suggesting shifts in forest communities toward fast-growing, low wood-density species (Joshi et al., 2023), while nutrient enrichment - another key global change driver - has been shown to reduce plant diversity across grasslands worldwide (Borer et al., 2014). Our results support this by showing that processes such as the balance between N uptake and resorption varying within PFTs, have measurable impacts on long-term C-N dynamics.

While PFT-based models offer a practical way to represent dominant vegetation types, being able to capture large-scale differences in vegetation structure, productivity, and biogeochemical cycling across biomes (Prentice et al., 2007), most LSMs that still rely on a small number of fixed PFTs and overlook functional diversity, may lead to biased C sink estimates at regional and global scales (Verheijen et al., 2015; Sakschewski et al., 2015; Fisher et al., 2015). Given the large uncertainties in global C sink projections in CMIP6 models (Arora et al., 2020; Friedlingstein et al., 2024), introducing more functional variation within PFTs or incorporating trait-based approaches could significantly improve predictions of C-nutrient interactions under climate change. Studies that include trait variation - by letting traits respond to climate or by

https://doi.org/10.5194/egusphere-2026-6138
Preprint. Discussion started: 2 November 2026
© Author(s) 2026. CC BY 4.0 License.

testing many different trait combinations - show that models capture vegetation-climate feedbacks more realistically and that communities remain more resilient to environmental change (Verheijen et al., 2013; Pavlick et al., 2013; Scheiter et al., 2013; Sakschewski et al., 2015). More recently, Wang et al. (2025) showed that going beyond PFTs to capture leaf trait variation by simulating diverse plant functional characteristics (PFC), can further improve vegetation representation in LSMs. Together, these studies highlight that adding functional variation is critical for more robust projections of ecosystem responses to global change.

4.4 Limitations and future directions

Although adjusting N uptake capacity parameter - that indirectly triggers a response in N resorption - successfully isolates the effects of N-use strategies within PFTs by holding e.g. phenology traits as constant, while we allow for dynamic allocation without altering other core trait dimensions, the model does not account for the continuous covariation in plant traits and their respective trade-offs that can interact with nutrient acquisition and retention strategies (Wright et al., 2004; Reich, 2014; Díaz et al., 2016).

Also, this study does not account for potential shifts in PFT composition under future climate, e.g., warming could lead to shifts of evergreen toward deciduous trees in boreal forests (Bonan, 2008) or drive broader biome changes through shifts in climate. Such shifts could affect both the discussed structural traits that determine C residence time, as well as the balance between N-use strategies, altering C-N dynamics and the capacity of the forest to act as C sink.

The experiment does not include interactions with other limiting nutrients such as P. Under rising CO_2, increased productivity could intensify P demand, constraining the capacity of plants to gain on additional C and N inputs (Peñuelas et al., 2013). Without considering P dynamics, the model may overestimate the potential for long-term C storage in P-limited regions, e.g. in the tropics, as nutrient co-limitation can alter both plant uptake responses, nutrient retention and therefore litter-soil feedbacks.

As most LSMs, the simulated future responses of soil N cycling processes depend strongly on the temperature sensitivity, particularly mineralization and biological N fixation. However, the extent to which future ecosystems will show proportionally strong increases in those processes remains uncertain. This study uses a simple representation of soil microbial processes and does not account for potential long-term shifts in microbial community composition or regional differences in microbial temperature optima, all could alter future N release rates. At present,

https://doi.org/10.5194/egusphere-2026-6138
Preprint. Discussion started: 2 November 2026
© Author(s) 2026. CC BY 4.0 License.

there are still limited data on how to represent future changes in microbial communities and their adaptation in global coupled C-N models.

Future developments for PFT-based models could focus on increasing the number and diversity of PFTs so that they better reflect the range of functional strategies found in real ecosystems. For example, rather than representing all broadleaf deciduous species with a single parameter set, models could differentiate types with fast nutrient uptake and turnover from those with slower, more conservative nutrient use. Another option is to move toward hybrid trait-based approaches that keep the computational efficiency of PFTs but allow certain plant traits to vary continuously within each PFT. This could help capture more of the functional diversity and ecological trade-offs that influence C-nutrient dynamics under the future climate (Fisher et al., 2015; Sakschewski et al., 2016; Lawrence et al., 2019). Even with its simplifications, this study shows that N-use strategies can meaningfully alter projections of C storage and that current PFT-only approaches in LSMs risk missing important within-PFT dynamics.

5. Conclusions

This study used a process-based model to explore how N-use strategies shape ecosystem C storage under future climate conditions. We show that broad-leaved deciduous with conservative N-use (higher N resorption) achieve the strongest relative advantage, combining higher gains in NPP and C storage with smaller rises in N losses, while needle-leaved evergreens with acquisitive N-use strategy (higher plant N uptake) hold the largest absolute C stocks. These effects are sustained and most pronounced in temperate and boreal regions, where the whole of N in limiting productivity increases. Together, our results suggest that while PFT traits determine the baseline for C storage, N-use strategies play a crucial role in modulating future trajectories of ecosystem N and C cycling. Accounting for variation in plant N-use strategies in land surface models is essential for improving predictions of ecosystem responses and the terrestrial C sink under climate change.

Data Availability Statement

The data that support the findings of this study are available in QS open access repository at https://doi.org/10.17871/quincy-model-2019. These data were derived from the following

https://doi.org/10.5194/egusphere-2026-6138
Preprint. Discussion started: 2 November 2026
© Author(s) 2026. CC BY 4.0 License.

resources available in the public domain: - QUINCY model - release 06, https://doi.org/10.17871/quincy-model-2019.

Author contributions

All authors designed the study. GS performed the analysis. All authors contributed to interpreting the results. GS drafted the manuscript; all authors contributed to writing and editing the manuscript.

Competing interests

BS is a member of the editorial board of Biogeosciences.

Acknowledgments

GMS acknowledges financial support from the IMPRS for Global Biogeochemical Cycles. SZ was supported by the European Union's 2020 research programme under grant agreement No 101003536 (ESM-2025). SC was funded by Research Ireland Frontiers for the Future grant no. 22/FFP-P/11474. This publication has emanated from research conducted with the financial support of Research Ireland, Northern Ireland's Department of Agriculture, Environment and Rural Affairs (DAERA), UK Research and Innovation (UKRI) via the International Science Partnerships Fund (ISPF) under Grant number [22/CC/11103] at the Co-Centre for Climate + Biodiversity + Water. We also receive philanthropic funding from the Sunflower Charitable Foundation and the Fernhill Fund at Community Foundation Ireland. Our Industry projects are part funded by our business partners.

6. References

Ainsworth, E. A. and Long, S. P.: What have we learned from 15 years of free-air CO2 enrichment (FACE)? A meta-analytic review of the responses of photosynthesis, canopy properties and plant production to rising CO2: Tansley review, New Phytol., 165, 351–371, https://doi.org/10.1111/j.1469-8137.2004.01224.x, 2005.

Arora, V. K., Katavouta, A., Williams, R. G., Jones, C. D., Brovkin, V., Friedlingstein, P., Schwinger, J., Bopp, L., Boucher, O., Cadule, P., Chamberlain, M. A., Christian, J. R., Delire,

https://doi.org/10.5194/egusphere-2026-6138
Preprint. Discussion started: 2 November 2026
© Author(s) 2026. CC BY 4.0 License.

C., Fisher, R. A., Hajima, T., Ilyina, T., Joetzjer, E., Kawamiya, M., Koven, C. D., Krasting, J. P., Law, R. M., Lawrence, D. M., Lenton, A., Lindsay, K., Pongratz, J., Raddatz, T., Séférian, R., Tachiiri, K., Tjiputra, J. F., Wiltshire, A., Wu, T., and Ziehn, T.: Carbon–concentration and carbon–climate feedbacks in CMIP6 models and their comparison to CMIP5 models, Biogeosciences, 17, 4173–4222, https://doi.org/10.5194/bg-17-4173-2020, 2020.

Bonan, G. B.: Forests and climate change: forcings, feedbacks, and the climate benefits of forests, Science, 320, 1444–1449, https://doi.org/10.1126/science.1155121, 2008.

Borer, E. T., Seabloom, E. W., Gruner, D. S., Harpole, W. S., Hillebrand, H., Lind, E. M., Adler, P. B., Alberti, J., Anderson, T. M., Bakker, J. D., Biederman, L., Blumenthal, D., Brown, C. S., Brudvig, L. A., Buckley, Y. M., Cadotte, M., Chu, C., Cleland, E. E., Crawley, M. J., Daleo, P., Damschen, E. I., Davies, K. F., DeCrappeo, N. M., Du, G., Firn, J., Hautier, Y., Heckman, R. W., Hector, A., HilleRisLambers, J., Iribarne, O., Klein, J. A., Knops, J. M. H., La Pierre, K. J., Leakey, A. D. B., Li, W., MacDougall, A. S., McCulley, R. L., Melbourne, B. A., Mitchell, C. E., Moore, J. L., Mortensen, B., O'Halloran, L. R., Orrock, J. L., Pascual, J., Prober, S. M., Pyke, D. A., Risch, A. C., Schuetz, M., Smith, M. D., Stevens, C. J., Sullivan, L. L., Williams, R. J., Wragg, P. D., Wright, J. P., and Yang, L. H.: Herbivores and nutrients control grassland plant diversity via light limitation, Nature, 508, 517–520, https://doi.org/10.1038/nature13144, 2014.

Bradford, M. A., Wieder, W. R., Bonan, G. B., Fierer, N., Raymond, P. A., and Crowther, T. W.: Managing uncertainty in soil carbon feedbacks to climate change, Nat. Clim. Chang., 6, 751–758, https://doi.org/10.1038/nclimate3071, 2016.

Cadotte, M. W.: Functional traits explain ecosystem function through opposing mechanisms, Ecol. Lett., 20, 989–996, https://doi.org/10.1111/ele.12796, 2017.

Caldararu, S., Thum, T., Yu, L., Kern, M., Nair, R., and Zaehle, S.: Long-term ecosystem nitrogen limitation from foliar δ15N data and a land surface model, Glob. Chang. Biol., 28, 493–508, https://doi.org/10.1111/gcb.15933, 2022.

https://doi.org/10.5194/egusphere-2026-6138
Preprint. Discussion started: 2 November 2026
© Author(s) 2026. CC BY 4.0 License.



Cambron, T. W., Fisher, J. B., Hungate, B. A., Stocker, B. D., Keenan, T., Prentice, I. C., and Terrer, C.: Plant nutrient acquisition under elevated CO2 and implications for the land carbon sink, Nat. Clim. Chang., 1–12, https://doi.org/10.1038/s41558-025-02386-y, 2025.

Chapin, F. S.: The Mineral Nutrition of Wild Plants, Annu. Rev. Ecol. Syst., 11, 233–260, https://doi.org/10.1146/annurev.es.11.110180.001313, 1980.

Cleveland, C. C., Houlton, B. Z., Smith, W. K., Marklein, A. R., Reed, S. C., Parton, W., Del Grosso, S. J., and Running, S. W.: Patterns of new versus recycled primary production in the terrestrial biosphere, Proc. Natl. Acad. Sci. U. S. A., 110, 12733–12737, https://doi.org/10.1073/pnas.1302768110, 2013.

Cucchi, M., Weedon, G. P., Amici, A., Bellouin, N., Lange, S., Müller Schmied, H., Hersbach, H., and Buontempo, C.: WFDE5: bias-adjusted ERA5 reanalysis data for impact studies, Earth Syst. Sci. Data, 12, 2097–2120, https://doi.org/10.5194/essd-12-2097-2020, 2020.

Díaz, S., Kattge, J., Cornelissen, J. H. C., Wright, I. J., Lavorel, S., Dray, S., Reu, B., Kleyer, M., Wirth, C., Prentice, I. C., Garnier, E., Bönisch, G., Westoby, M., Poorter, H., Reich, P. B., Moles, A. T., Dickie, J., Gillison, A. N., Zanne, A. E., Chave, J., Wright, S. J., Sheremet'ev, S. N., Jactel, H., Baraloto, C., Cerabolini, B., Pierce, S., Shipley, B., Kirkup, D., Casanoves, F., Joswig, J. S., Günther, A., Falczuk, V., Rüger, N., Mahecha, M. D., and Gorné, L. D.: The global spectrum of plant form and function, Nature, 529, 167–171, https://doi.org/10.1038/nature16489, 2016.

Díaz, S. and Cabido, M.: Vive la différence: plant functional diversity matters to ecosystem processes, Trends Ecol. Evol., 16, 646–655, https://doi.org/10.1016/s0169-5347(01)02283-2, 2001.

Finzi, A. C., Norby, R. J., Calfapietra, C., Gallet-Budynek, A., Gielen, B., Holmes, W. E., Hoosbeek, M. R., Iversen, C. M., Jackson, R. B., Kubiske, M. E., Ledford, J., Liberloo, M., Oren, R., Polle, A., Pritchard, S., Zak, D. R., Schlesinger, W. H., and Ceulemans, R.: Increases in nitrogen uptake rather than nitrogen-use efficiency support higher rates of temperate forest

https://doi.org/10.5194/egusphere-2026-6138
Preprint. Discussion started: 2 November 2026
© Author(s) 2026. CC BY 4.0 License.

774 productivity under elevated CO_2, Proc. Natl. Acad. Sci. U. S. A., 104, 14014–14019,
775 https://doi.org/10.1073/pnas.0706518104, 2007.
776
777 Fisher, R. A. and Koven, C. D.: Perspectives on the future of land surface models and the
778 challenges of representing complex terrestrial systems, J. Adv. Model. Earth Syst., 12,
779 e2018MS001453, https://doi.org/10.1029/2018ms001453, 2020.
780
781 Fisher, R. A., Muszala, S., Verteinstein, M., Lawrence, P., Xu, C., McDowell, N. G., Knox, R.
782 G., Koven, C., Holm, J., Rogers, B. M., Spessa, A., Lawrence, D., and Bonan, G.: Taking off
783 the training wheels: the properties of a dynamic vegetation model without climate envelopes,
784 CLM4.5(ED), Geosci. Model Dev., 8, 3593–3619, https://doi.org/10.5194/gmd-8-3593-2015,
785 2015.
786
787 Grime, J. P.: Benefits of plant diversity to ecosystems: immediate, filter and founder effects, J.
788 Ecol., 86, 902–910, https://doi.org/10.1046/j.1365-2745.1998.00306.x, 1998.
789
790 Hedin, L. O., Brookshire, E. N. J., Menge, D. N. L., and Barron, A. R.: The Nitrogen Paradox
791 in Tropical Forest Ecosystems, Annu. Rev. Ecol. Evol. Syst., 40, 613–635,
792 https://doi.org/10.1146/annurev.ecolsys.37.091305.110246, 2009.
793
794 Joshi, J., Hofhansl, F., Singh, S., Stocker, B. D., Brännström, Å., Franklin, O., Blanco, C. C.,
795 Aleixo, I. F., Lapola, D., Prentice, I. C., and Dieckmann, U.: Competition for light can drive
796 adverse species-composition shifts in the Amazon Forest under elevated CO2, bioRxiv
797 [preprint], https://doi.org/10.1101/2023.07.03.547575, 2023.
798
799 Lange, S.: Trend-preserving bias adjustment and statistical downscaling with ISIMIP3BASD
800 (v1.0), Geosci. Model Dev., 12, 3055–3070, https://doi.org/10.5194/gmd-12-3055-2019, 2019.
801
802 Luo, Y., Su, B., Currie, W. S., Dukes, J. S., Finzi, A., Hartwig, U., Hungate, B., McMurtrie, R.
803 E., Oren, R., Parton, W. J., Pataki, D. E., Shaw, R. M., Zak, D. R., and Field, C. B.: Progressive
804 nitrogen limitation of ecosystem responses to rising atmospheric carbon dioxide, BioScience,
805 54, 731–739, https://doi.org/10.1641/0006-3568(2004)054[0731:PNLOER]2.0.CO;2, 2004.

https://doi.org/10.5194/egusphere-2026-6138
Preprint. Discussion started: 2 November 2026
© Author(s) 2026. CC BY 4.0 License.

McPartland, M. Y., Montgomery, R. A., Hanson, P. J., Phillips, J. R., Kolka, R., and Palik, B.: Vascular plant species response to warming and elevated carbon dioxide in a boreal peatland, Environ. Res. Lett., 15, 124066, https://doi.org/10.1088/1748-9326/abc4fb, 2020.

Meinshausen, M., Nicholls, Z. R. J., Lewis, J., Gidden, M. J., Vogel, E., Freund, M., Beyerle, U., Gessner, C., Nauels, A., Bauer, N., Canadell, J. G., Daniel, J. S., John, A., Krummel, P. B., Luderer, G., Meinshausen, N., Montzka, S. A., Rayner, P. J., Reimann, S., Smith, S. J., van den Berg, M., Velders, G. J. M., Vollmer, M. K., and Wang, R. H. J.: The shared socio-economic pathway (SSP) greenhouse gas concentrations and their extensions to 2500, Geosci. Model Dev., 13, 3571–3605, https://doi.org/10.5194/gmd-13-3571-2020, 2020.

Melillo, J. M., Butler, S., Johnson, J., Mohan, J., Steudler, P., Lux, H., Burrows, E., Bowles, F., Smith, R., Scott, L., Vario, C., Hill, T., Burton, A., Zhou, Y.-M., and Tang, J.: Soil warming, carbon-nitrogen interactions, and forest carbon budgets, Proc. Natl. Acad. Sci. U. S. A., 108, 9508–9512, https://doi.org/10.1073/pnas.1018189108, 2011.

Norby, R. J. and Zak, D. R.: Ecological lessons from free-air CO2 enrichment (FACE) experiments, Annu. Rev. Ecol. Evol. Syst., 42, 181–203, https://doi.org/10.1146/annurev-ecolsys-102209-144647, 2011.

Norby, R. J., Delucia, E. H., Gielen, B., Calfapietra, C., Giardina, C. P., King, J. S., Ledford, J., McCarthy, H. R., Moore, D. J. P., Ceulemans, R., De Angelis, P., Finzi, A. C., Karnosky, D. F., Kubiske, M. E., Lukac, M., Pregitzer, K. S., Scarascia-Mugnozza, G. E., Schlesinger, W. H., and Oren, R.: Forest response to elevated CO2 is conserved across a broad range of productivity, Proc. Natl. Acad. Sci. U. S. A., 102, 18052–18056, https://doi.org/10.1073/pnas.0509478102, 2005.

Peñuelas, J., Poulter, B., Sardans, J., Ciais, P., van der Velde, M., Bopp, L., Boucher, O., Godderis, Y., Hinsinger, P., Llusia, J., Nardin, E., Vicca, S., Obersteiner, M., and Janssens, I. A.: Human-induced nitrogen-phosphorus imbalances alter natural and managed ecosystems across the globe, Nat. Commun., 4, 2934, https://doi.org/10.1038/ncomms3934, 2013.

https://doi.org/10.5194/egusphere-2026-6138
Preprint. Discussion started: 2 November 2026
© Author(s) 2026. CC BY 4.0 License.

Phillips, R. P., Brzostek, E., and Midgley, M. G.: The mycorrhizal-associated nutrient economy: a new framework for predicting carbon-nutrient couplings in temperate forests, New Phytol., 199, 41–51, https://doi.org/10.1111/nph.12221, 2013.

Prentice, I. C., Bondeau, A., Cramer, W., Harrison, S. P., Hickler, T., Lucht, W., Sitch, S., Smith, B., and Sykes, M. T.: Dynamic global vegetation modeling: Quantifying terrestrial ecosystem responses to large-scale environmental change, in: Terrestrial Ecosystems in a Changing World, Springer Berlin Heidelberg, Berlin, Heidelberg, 175–192, https://doi.org/10.1007/978-3-540-32730-1_15, 2007.

Reich, P. B.: The world-wide 'fast-slow' plant economics spectrum: a traits manifesto, J. Ecol., 102, 275–301, https://doi.org/10.1111/1365-2745.12211, 2014.

Sakschewski, B., von Bloh, W., Boit, A., Poorter, L., Peña-Claros, M., Heinke, J., Joshi, J., and Thonicke, K.: Resilience of Amazon forests emerges from plant trait diversity, Nat. Clim. Chang., 6, 1032–1036, https://doi.org/10.1038/nclimate3109, 2016.

San Román, A. X., Srikanthan, N., Hamid, A. A., Muratore, T. J., Knorr, M. A., Frey, S. D., and Simpson, M. J.: Long-term warming in a temperate forest accelerates soil organic matter decomposition despite increased plant-derived inputs, Biogeochemistry, 167, 1159–1174, https://doi.org/10.1007/s10533-024-01165-9, 2024.

Schmidt, M. W. I., Torn, M. S., Abiven, S., Dittmar, T., Guggenberger, G., Janssens, I. A., Kleber, M., Kögel-Knabner, I., Lehmann, J., Manning, D. A. C., Nannipieri, P., Rasse, D. P., Weiner, S., and Trumbore, S. E.: Persistence of soil organic matter as an ecosystem property, Nature, 478, 49–56, https://doi.org/10.1038/nature10386, 2011.

Sellar, A. A., Jones, C. G., Mulcahy, J. P., Tang, Y., Yool, A., Wiltshire, A., O'Connor, F. M., Stringer, M., Hill, R., Palmieri, J., Woodward, S., Mora, L., Kuhlbrodt, T., Rumbold, S. T., Kelley, D. I., Ellis, R., Johnson, C. E., Walton, J., Abraham, N. L., Andrews, M. B., Andrews, T., Archibald, A. T., Berthou, S., Burke, E., Blockley, E., Carslaw, K., Dalvi, M., Edwards, J.,

https://doi.org/10.5194/egusphere-2026-6138
Preprint. Discussion started: 2 November 2026
© Author(s) 2026. CC BY 4.0 License.

Folberth, G. A., Gedney, N., Griffiths, P. T., Harper, A. B., Hendry, M. A., Hewitt, A. J., Johnson, B., Jones, A., Jones, C. D., Keeble, J., Liddicoat, S., Morgenstern, O., Parker, R. J., Predoi, V., Robertson, E., Siahaan, A., Smith, R. S., Swaminathan, R., Woodhouse, M. T., Zeng, G., and Zerroukat, M.: UKESM1: Description and evaluation of the U.k. earth system model, J. Adv. Model. Earth Syst., 11, 4513–4558, https://doi.org/10.1029/2019ms001739, 2019.

Sistla, S. A., Moore, J. C., Simpson, R. T., Gough, L., Shaver, G. R., and Schimel, J. P.: Long-term warming restructures Arctic tundra without changing net soil carbon storage, Nature, 497, 615–618, https://doi.org/10.1038/nature12129, 2013.

Sophia, G., Caldararu, S., Stocker, B. D., and Zaehle, S.: Dynamic nitrogen resorption improves predictions of nitrogen cycling responses to global change in a next generation ecosystem model, J. Adv. Model. Earth Syst., 18, e2025MS005181, https://doi.org/10.1029/2025MS005181, 2026.

Stocker, B. D., Dong, N., Perkowski, E. A., Schneider, P. D., Xu, H., de Boer, H. J., Rebel, K. T., Smith, N. G., Van Sundert, K., Wang, H., Jones, S. E., Prentice, I. C., and Harrison, S. P.: Empirical evidence and theoretical understanding of ecosystem carbon and nitrogen cycle interactions, New Phytol., 245, 49–68, https://doi.org/10.1111/nph.20178, 2025.

Terrer, C., Jackson, R. B., Prentice, I. C., Keenan, T. F., Kaiser, C., Vicca, S., Fisher, J. B., Reich, P. B., Stocker, B. D., Hungate, B. A., Peñuelas, J., McCallum, I., Soudzilovskaia, N. A., Cernusak, L. A., Talhelm, A. F., Van Sundert, K., Piao, S., Newton, P. C. D., Hovenden, M. J., Blumenthal, D. M., Liu, Y. Y., Müller, C., Winter, K., Field, C. B., Viechtbauer, W., Van Lissa, C. J., Hoosbeek, M. R., Watanabe, M., Koike, T., Leshyk, V. O., Polley, H. W., and Franklin, O.: Nitrogen and phosphorus constrain the CO2 fertilization of global plant biomass, Nat. Clim. Chang., 9, 684–689, https://doi.org/10.1038/s41558-019-0545-2, 2019.

Thum, T., Caldararu, S., Engel, J., Kern, M., Pallandt, M., Schnur, R., Yu, L., and Zaehle, S.: A new model of the coupled carbon, nitrogen, and phosphorus cycles in the terrestrial biosphere

https://doi.org/10.5194/egusphere-2026-6138
Preprint. Discussion started: 2 November 2026
© Author(s) 2026. CC BY 4.0 License.

(QUINCY v1.0; revision 1996), Geosci. Model Dev., 12, 4781–4802, https://doi.org/10.5194/gmd-12-4781-2019, 2019.

Van Bodegom, P. M., Douma, J. C., Witte, J. P. M., Ordoñez, J. C., Bartholomeus, R. P., and Aerts, R.: Going beyond limitations of plant functional types when predicting global ecosystem–atmosphere fluxes: exploring the merits of traits-based approaches: Merits of traits-based vegetation modelling, Glob. Ecol. Biogeogr., 21, 625–636, https://doi.org/10.1111/j.1466-8238.2011.00717.x, 2012.

Verheijen, L. M., Brovkin, V., Aerts, R., Bönisch, G., Cornelissen, J. H. C., Kattge, J., Reich, P. B., Wright, I. J., and van Bodegom, P. M.: Impacts of trait variation through observed trait–climate relationships on performance of an Earth system model: a conceptual analysis, Biogeosciences, 10, 5497–5515, https://doi.org/10.5194/bg-10-5497-2013, 2013.

Vitousek, P. M., Porder, S., Houlton, B. Z., and Chadwick, O. A.: Terrestrial phosphorus limitation: mechanisms, implications, and nitrogen-phosphorus interactions, Ecol. Appl., 20, 5–15, https://doi.org/10.1890/08-0127.1, 2010.

Walker, A. P., De Kauwe, M. G., Bastos, A., Belmecheri, S., Georgiou, K., Keeling, R. F., McMahon, S. M., Medlyn, B. E., Moore, D. J. P., Norby, R. J., Zaehle, S., Anderson-Teixeira, K. J., Battipaglia, G., Brienen, R. J. W., Cabugao, K. G., Cailleret, M., Campbell, E., Canadell, J. G., Ciais, P., Craig, M. E., Ellsworth, D. S., Farquhar, G. D., Fatichi, S., Fisher, J. B., Frank, D. C., Graven, H., Gu, L., Haverd, V., Heilman, K., Heimann, M., Hungate, B. A., Iversen, C. M., Joos, F., Jiang, M., Keenan, T. F., Knauer, J., Körner, C., Leshyk, V. O., Leuzinger, S., Liu, Y., MacBean, N., Malhi, Y., McVicar, T. R., Penuelas, J., Pongratz, J., Powell, A. S., Riutta, T., Sabot, M. E. B., Schleucher, J., Sitch, S., Smith, W. K., Sulman, B., Taylor, B., Terrer, C., Torn, M. S., Treseder, K. K., Trugman, A. T., Trumbore, S. E., van Mantgem, P. J., Voelker, S. L., Whelan, M. E., and Zuidema, P. A.: Integrating the evidence for a terrestrial carbon sink caused by increasing atmospheric CO2, New Phytol., 229, 2413–2445, https://doi.org/10.1111/nph.16866, 2021.

https://doi.org/10.5194/egusphere-2026-6138
Preprint. Discussion started: 2 November 2026
© Author(s) 2026. CC BY 4.0 License.

Walker, T. W. and Syers, J. K.: The fate of phosphorus during pedogenesis, Geoderma, 15, 1–19, https://doi.org/10.1016/0016-7061(76)90066-5, 1976.

Wang, Y., Braghiere, R. K., Fischer, W. W., Yao, Y., Shen, Z., Schneider, T., Bloom, A. A., Schimel, D., Croft, H., Winkler, A. J., Reichstein, M., and Frankenberg, C.: Impacts of leaf traits on vegetation optical properties in Earth system modeling, Nat. Commun., 16, 4968, https://doi.org/10.1038/s41467-025-60149-x, 2025.

Wieder, W. R., Cleveland, C. C., Smith, W. K., and Todd-Brown, K.: Future productivity and carbon storage limited by terrestrial nutrient availability, Nat. Geosci., 8, 441–444, https://doi.org/10.1038/ngeo2413, 2015.

Wieners, K.-H., Giorgetta, M., Jungclaus, J., Reick, C., Esch, M., Bittner, M., Legutke, S., Schupfner, M., Wachsmann, F., Gayler, V., Haak, H., de Vrese, P., Raddatz, T., Mauritsen, T., von Storch, J.-S., Behrens, J., Brovkin, V., Claussen, M., Crueger, T., Fast, I., Fiedler, S., Hagemann, S., Hohenegger, C., Jahns, T., Kloster, S., Kinne, S., Lasslop, G., Kornblueh, L., Marotzke, J., Matei, D., Meraner, K., Mikolajewicz, U., Modali, K., Müller, W., Nabel, J., Notz, D., Peters-von Gehlen, K., Pincus, R., Pohlmann, H., Pongratz, J., Rast, S., Schmidt, H., Schnur, R., Schulzweida, U., Six, K., Stevens, B., Voigt, A., and Roeckner, E.: MPI-M MPI-ESM1.2-LR model output prepared for CMIP6 CMIP historical, https://doi.org/10.22033/ESGF/CMIP6.6595, 2019.

Wright, I. J., Reich, P. B., Westoby, M., Ackerly, D. D., Baruch, Z., Bongers, F., Cavender-Bares, J., Chapin, T., Cornelissen, J. H. C., Diemer, M., Flexas, J., Garnier, E., Groom, P. K., Gulias, J., Hikosaka, K., Lamont, B. B., Lee, T., Lee, W., Lusk, C., Midgley, J. J., Navas, M.-L., Niinemets, U., Oleksyn, J., Osada, N., Poorter, H., Poot, P., Prior, L., Pyankov, V. I., Roumet, C., Thomas, S. C., Tjoelker, M. G., Veneklaas, E. J., and Villar, R.: The worldwide leaf economics spectrum, Nature, 428, 821–827, https://doi.org/10.1038/nature02403, 2004.

Zaehle, S. and Friend, A. D.: Carbon and nitrogen cycle dynamics in the O-CN land surface model: 1. Model description, site-scale evaluation, and sensitivity to parameter estimates:

https://doi.org/10.5194/egusphere-2026-6138
Preprint. Discussion started: 2 November 2026
© Author(s) 2026. CC BY 4.0 License.



SITE-SCALE EVALUATION OF A C-N MODEL, Global Biogeochem. Cycles, 24, https://doi.org/10.1029/2009gb003521, 2010.

Zaehle, S., Friedlingstein, P., and Friend, A. D.: Terrestrial nitrogen feedbacks may accelerate future climate change: CARBON-NITROGEN FEEDBACKS AFFECT CLIMATE, Geophys. Res. Lett., 37, https://doi.org/10.1029/2009gl041345, 2010.

Zaehle, S., Jones, C. D., Houlton, B., Lamarque, J.-F., and Robertson, E.: Nitrogen availability reduces CMIP5 projections of twenty-first-century land carbon uptake, J. Clim., 28, 2494–2511, https://doi.org/10.1175/jcli-d-13-00776.1, 2015.

Zhu, J., Jia, Y., Yu, G., Wang, Q., He, N., Chen, Z., He, H., Zhu, X., Li, P., Zhang, F., Liu, X., Goulding, K., Fowler, D., and Vitousek, P.: Changing patterns of global nitrogen deposition driven by socio-economic development, Nat. Commun., 16, 46, https://doi.org/10.1038/s41467-024-55606-y, 2025.

https://doi.org/10.5194/egusphere-2026-6138
Preprint. Discussion started: 2 November 2026
© Author(s) 2026. CC BY 4.0 License.

Appendix A: Detailed model description and sensitivity

A1 - Vmax parameter sensitivity

To assess the sensitivity of plant nitrogen (N) uptake capacity on the plant productivity, we performed a parameter sensitivity analysis by varying the maximum N uptake rate (v_{max}) across a ±40% range around its default value (0.42) in 10% increase and decrease (Table A1; Fig. A1). This setup allowed us to identify the largest change in N uptake capacity that does not strongly compromise plant survival compared to the default configuration. We excluded sites with GPP below 500 gC/m^2/yr in the default run, as such low productivity is not representative of forest vegetation. For this study, we selected the ±20% sensitivity level, which showed an effect on GPP while avoiding substantial site loss under conservative strategies compared to the default configuration.

Table A1. Parameter sensitivity values for maximum N uptake rate (v_{max}).

Run name	Change (%)	v_{max} value
conservative_40	-40%	0.25
conservative_30	-30%	0.29
conservative_20	-20%	0.33
conservative_10	-10%	0.37
default	0%	0.42
acquisitive_10	+10%	0.46
acquisitive_20	+20%	0.50
acquisitive_30	+30%	0.54
acquisitive_40	+40%	0.58

https://doi.org/10.5194/egusphere-2026-6138
Preprint. Discussion started: 2 November 2026
© Author(s) 2026. CC BY 4.0 License.

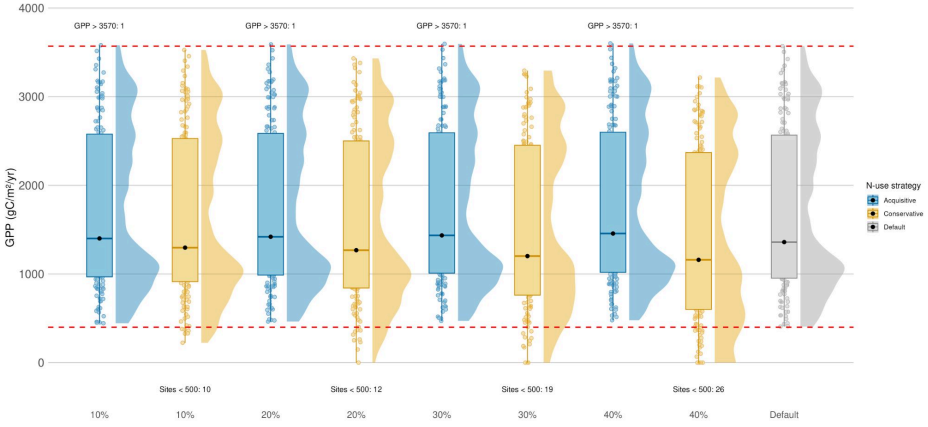
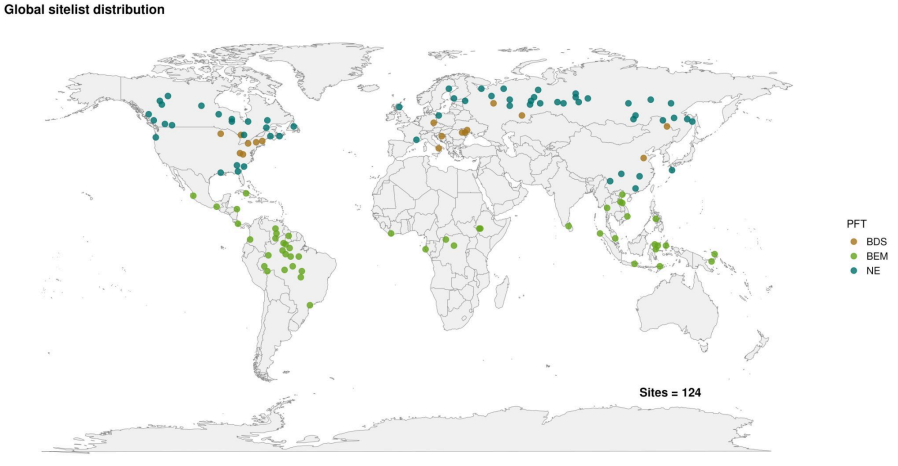


Figure A1: Site-level Gross Primary Productivity (GPP) for the Default model configuration (gray) and sensitivity experiments with ±10%, ±20%, ±30%, and ±40% changes in v_{max}, where blue shows acquisitive N-use strategy (higher v_{max}) and orange shows conservative N-use (lower v_{max}) responses. Boxplots display the median (black dots), interquartile range, and outliers, with side density plots illustrating the overall distribution of values within each group. Dashed red lines indicate GPP thresholds of 500 gC/m^2/yr (low productivity) and 3570 gC/m^2/yr (high productivity, above the maximum GPP in the Default run). Labels report the number of sites falling below or above these thresholds for each scenario.

A2 - Site selection for the first comparative experiment



https://doi.org/10.5194/egusphere-2026-6138
Preprint. Discussion started: 2 November 2026
© Author(s) 2026. CC BY 4.0 License.

Figure A2: Global sitelist distribution with its original PFT assignment. Each point corresponds to a site and colors represent different plant functional types (PFT). Moist broadleaved evergreen (BEM), summer green broadleaved deciduous (BDS) and needle-leaves evergreen (NE). Total number of sites = 124.

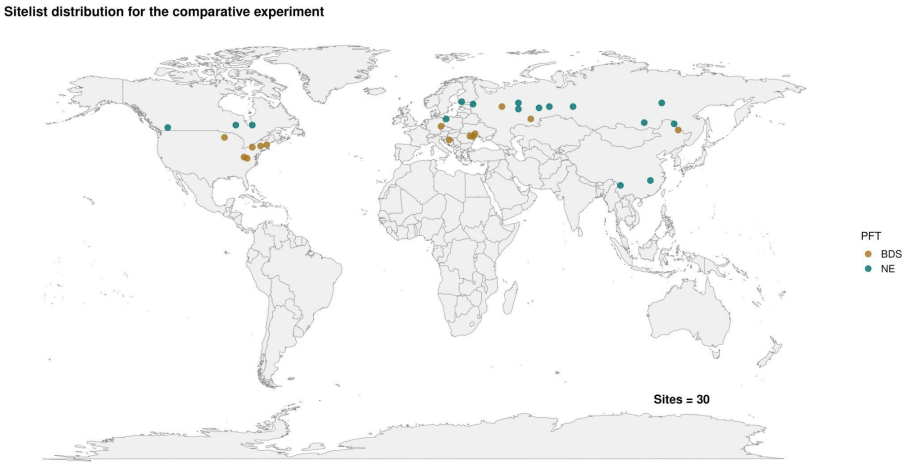


Figure A3: Sitelist distribution for the comparative experiment with its original PFT assignment. Each point corresponds to a site and colors represent different plant functional types (PFT). Summer green broadleaved deciduous (BDS) and needle-leaves evergreen (NE). Total number of sites = 30.

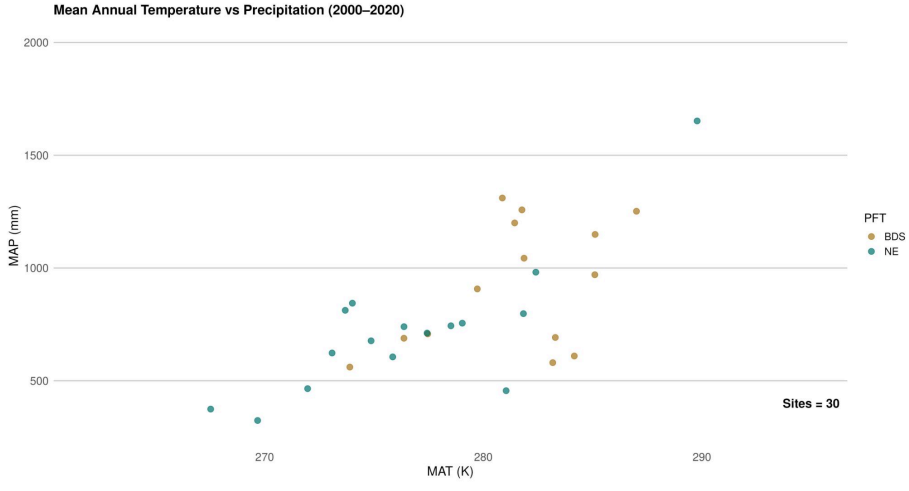


Figure A4: Climate distribution of sites for the comparative experiment, represented by Mean Annual Precipitation (MAP; mm) and Mean Annual Temperature (MAT; K) for the present day (2000-2020). Each point

https://doi.org/10.5194/egusphere-2026-6138
Preprint. Discussion started: 2 November 2026
© Author(s) 2026. CC BY 4.0 License.

corresponds to a site and illustrates the range of climatic conditions in the selected dataset. Total number of sites = 30.

Appendix B: Additional figures for the comparative and global experiments

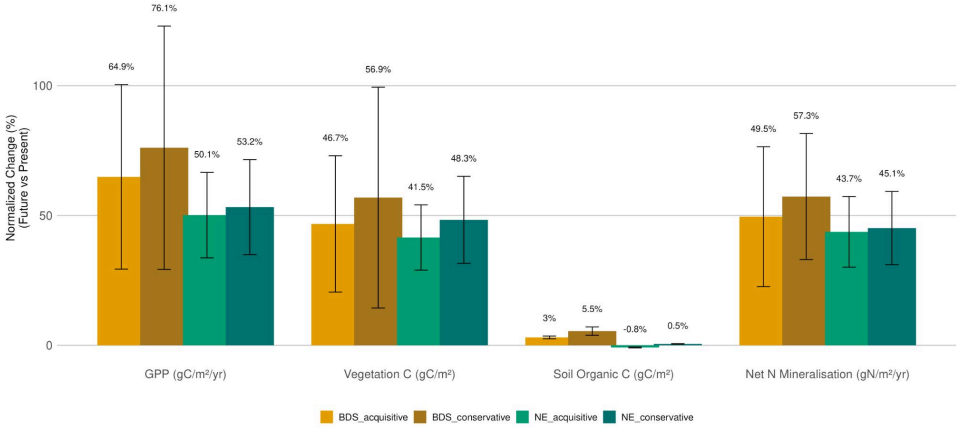


Figure B1: Normalized Change (%) between Future and Present day for Gross Primary Productivity (GPP; $gN/m^2/yr$), Vegetation carbon (C) (gC/m^2), Soil Organic C (gC/m^2) and Net N Mineralization ($gN/m^2/yr$). Bars represent the percent normalized difference and error bars indicate the propagated standard deviation (SE). Different colors show simulations for each plant functional type (broad-leaved deciduous [BDS] and needle-leaved evergreen [NE]) under acquisitive and conservative N-use strategies.

https://doi.org/10.5194/egusphere-2026-6138
Preprint. Discussion started: 2 November 2026
© Author(s) 2026. CC BY 4.0 License.

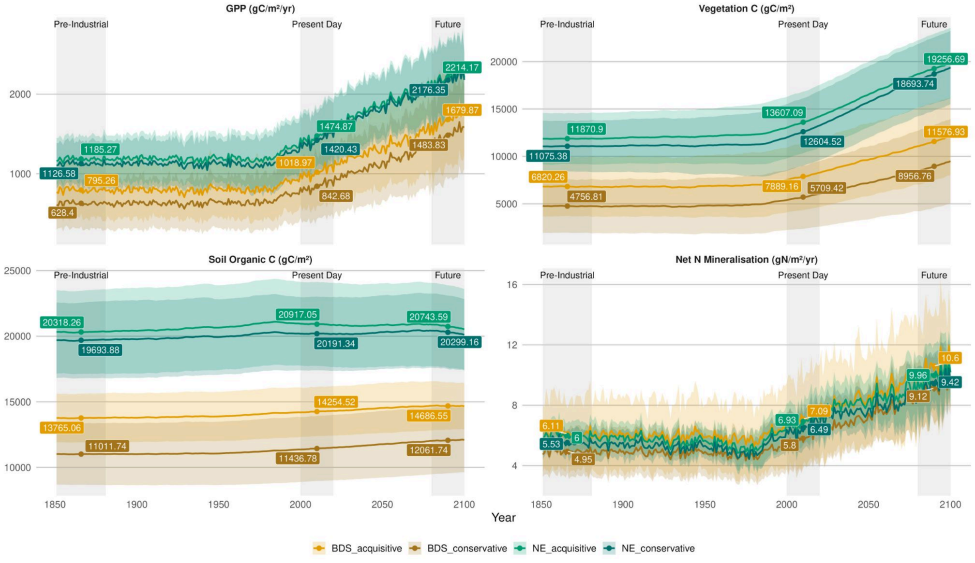


Figure B2: Temporal trends of GPP (Gross Primary Productivity; gC/m^2/yr), Vegetation carbon (C) (gC/m^2), Soil Organic C (gC/m^2), and Net nitrogen (N) Mineralization (gN/m^2/yr) from 1850 to 2100, based on ISIMIP3b UKESM climate forcing, for the comparative experiment. Different colors show simulations for each plant functional type (broad-leaved deciduous [BDS] and needle-leaved evergreen [NE]) under acquisitive and conservative N-use strategies. The shaded area represents the standard deviation across the 30 sites. Values represent mean annual estimates for each defined period: pre-industrial (1850-1880), present-day (2000-2020), and future (2080-2100).

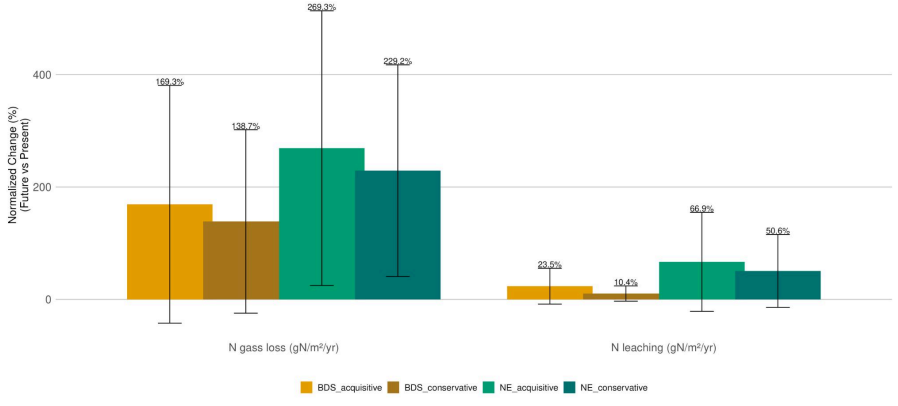


Figure B3: Normalized Change (%) between Future and Present day for N gas loss (gN/m^2/yr) and N leaching (gN/m^2/yr). Bars represent the percent normalized difference and error bars indicate the propagated standard

https://doi.org/10.5194/egusphere-2026-6138
Preprint. Discussion started: 2 November 2026
© Author(s) 2026. CC BY 4.0 License.

deviation (SE). Different colors show simulations for each plant functional type (broad-leaved deciduous [BDS] and needle-leaved evergreen [NE]) under acquisitive and conservative N-use strategies.

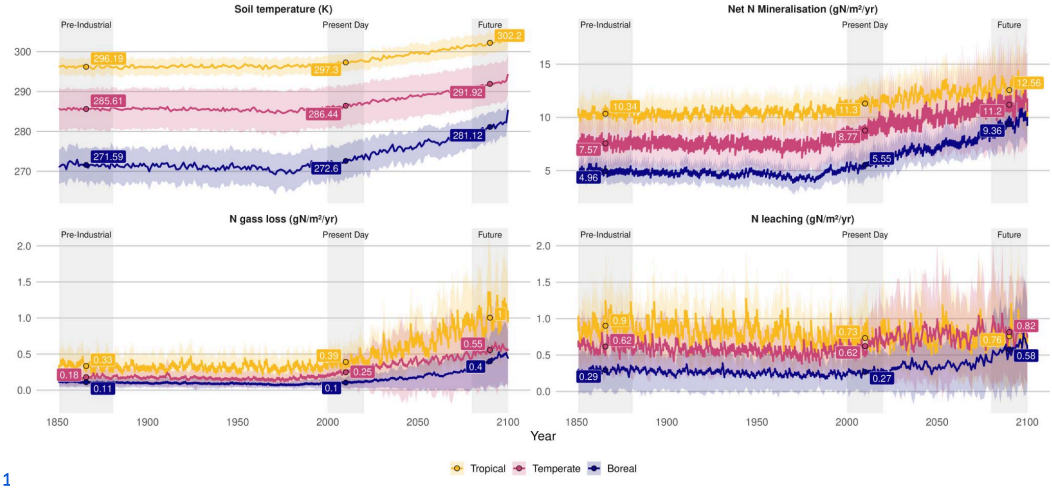
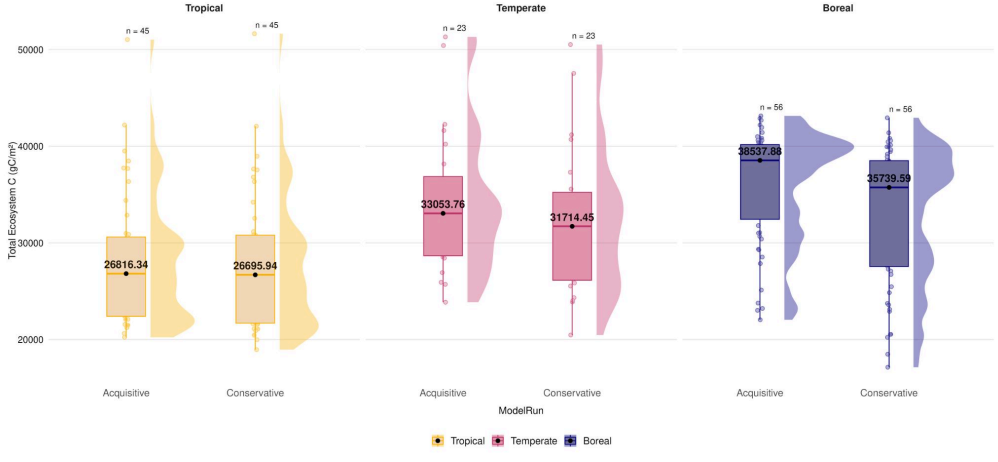


Figure B4: Temporal trends of Soil temperature (K), Net N Mineralization (gN/m^2/yr), N gass loss (gN/m^2/yr) and N leaching (gN/m^2/yr) from 1850 to 2100, based on ISIMIP3b UKESM climate forcing. Different colors show different climate zones (Tropical, Temperate, Boreal). Shaded area represents the standard deviation across the 124 global sites. Values represent mean annual estimates for each defined period: pre-industrial (1850-1880), present-day (2000-2020), and future (2080-2100).



https://doi.org/10.5194/egusphere-2026-6138
Preprint. Discussion started: 2 November 2026
© Author(s) 2026. CC BY 4.0 License.

Figure B5: Boxplots show the global distribution of total ecosystem carbon (C) storage (gC/m²) across climate zones, for the future period 2080-2100 under two nitrogen-use strategies (acquisitive and conservative). Sites are grouped by Köppen climate classification in Tropical, Temperate, and Boreal zones. Boxplots display the median (black dots), interquartile range, and outliers, with side density plots illustrating the overall distribution of values within each group. The number of observations (n) is shown above each box.

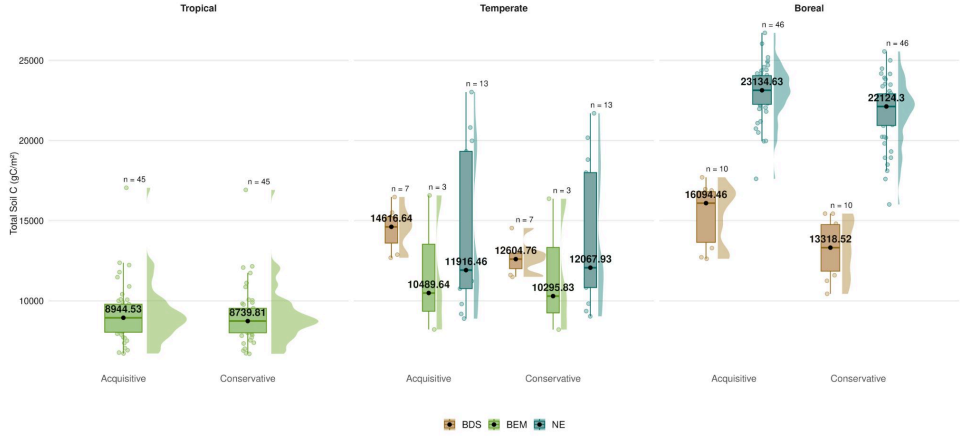


Figure B6: Boxplots show the global distribution of Total Soil carbon (C) storage (gC/m²) across climate zones and plant functional types (PFTs), for the future period 2080-2100 under two nitrogen-use strategies (acquisitive and conservative). Sites are grouped by Köppen climate classification in Tropical, Temperate, and Boreal zones. Different colors represent each PFT: broad-leaved deciduous (BDS), broad-leaved evergreen (BEM), and needle-leaved evergreen (NE). Boxplots display the median (black dots), interquartile range, and outliers, with side density plots illustrating the overall distribution of values within each group. The number of observations (n) is shown above each box.

https://doi.org/10.5194/egusphere-2026-6138
Preprint. Discussion started: 2 November 2026
© Author(s) 2026. CC BY 4.0 License.

Appendix C: MPI climate forcing sensitivity

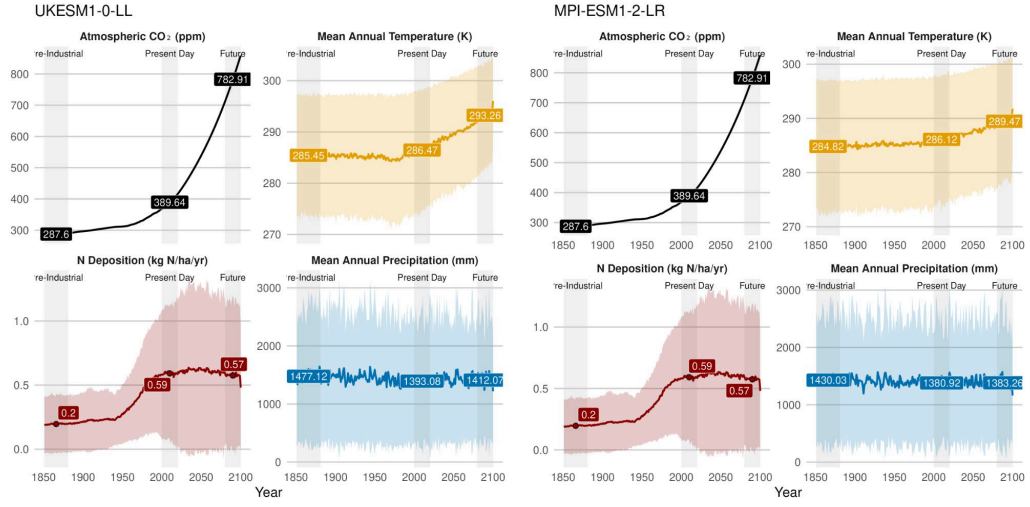


Figure C1: Climate trajectory of atmospheric CO_2 (ppm), Mean Annual Temperature (K), N Deposition (kgN ha/yr) and Mean Annual Precipitation (mm) for the global experiment (124 sites), comparing UKESM1-0-LL and MPI-ESM1-2-LR climate models. Pre-industrial (1850-1880), present-day (2000-2020), and future (2080-2100).

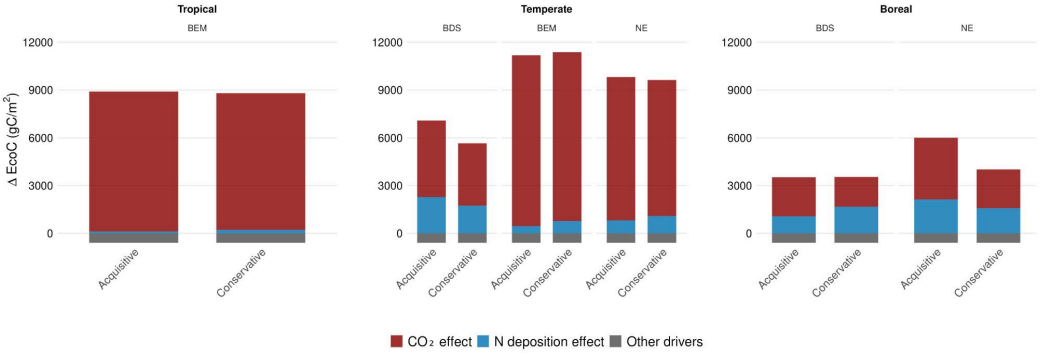


Figure C2: Bars show the change in total ecosystem carbon (ΔEcoC; Future - Present day) separated by N-use strategy and plant functional type (PFT) within each climate zone, using the MPI climate model. Colors indicate the estimated contribution from each driver: N deposition, CO_2, and other drivers. Driver contributions were calculated by comparing the normal run (all factors varying) with experimental runs where either CO_2 concentration or N deposition was held constant. CO_2 effect = ΔEcoC(normal) - ΔEcoC(CO_2 fixed); N deposition effect = ΔEcoC(normal) - ΔEcoC(N deposition fixed); Other drivers = ΔEcoC(normal) - (CO_2 effect + N deposition effect).